HHS Public Access

Author manuscript

Nat Commun. Author manuscript; available in PMC 2019 June 18.

Published in final edited form as:

Nat Commun. ; 5: 5217. doi:10.1038/ncomms6217.

RNAi-based functional selection identifies novel cell migration determinants dependent on PI3K and AKT pathways

Minchul Seo[1,2,#], **Shinrye Lee**[1,3,#], **Jong-Heon Kim**[1], **Won-Ha Lee**[4], **Guang Hu**[5], **Stephen J. Elledge**[6], and **Kyoungho Suk**[1,*]

[1]Department of Pharmacology, Brain Science & Engineering Institute, BK21 Plus KNU Biomedical Convergence Program, Kyungpook National University School of Medicine, Daegu, Republic of Korea

[2]College of Medicine, Dongguk University, Gyeongju, Republic of Korea

[3]Korea Brain Research Institute (KBRI), Daegu, Republic of Korea

[4]School of Life Sciences and Biotechnology, KNU Creative BioResearch Group, Kyungpook National University, Daegu, Republic of Korea

[5]Laboratory of Molecular Carcinogenesis, National Institute of Environmental Health and Sciences, Research Triangle Park, NC 27709, USA

[6]Department of Genetics, Howard Hughes Medical Institute, Division of Genetics, Brigham and Women's Hospital, Harvard Medical School, Boston, MA 02115, USA.

Abstract

Lentiviral short hairpin RNA (shRNA)-mediated genetic screening is a powerful tool for identifying loss-of-function phenotype in mammalian cells. Here, we report the identification of 91 cell migration-regulating genes using unbiased genome-wide functional genetic selection. Individual knockdown or cDNA overexpression of a set of 10 candidates reveals that most of these cell migration determinants are strongly dependent on PI3K/PTEN/AKT pathway and on their downstream signals, such as FOXO1 and p70S6K1. ALK, one of the cell migration promoting genes, uniquely uses p55γ regulatory subunit of PI3K, rather than more common p85 subunit, to trigger the activation of PI3K-AKT pathway. Our method enables the rapid and cost-effective genome-wide selection of cell migration regulators. Our results emphasize the importance of the PI3K/PTEN/AKT pathway as a point of convergence for multiple regulators of cell migration.

*To whom correspondence should be addressed: Department of Pharmacology, Kyungpook National University School of Medicine, 680 Gukchaebosang Street, Joong-gu, Daegu, 700-422, Republic of Korea. Phone: 82-53-420-4835. Fax: 82-53-256-1566. ksuk@knu.ac.kr.

Author contributions

M.S and S.L performed the experiments, analyzed the data, and prepared the manuscript. J.K performed the biochemical assays. W.L. analyzed the data. G.H and S.J.E provided reagents and analyzed the data. K.S directed the study and were involved in all aspects of the experimental design, data analysis and manuscript preparation. All authors critically reviewed the text and figures.

#These authors equally contributed to this work.

Competing financial interests

The authors declare no competing financial interests.

Introduction

Cell migration is a dynamic process that requires coordinated cytoskeletal regulation and proper polarization, and is governed by the extracellular microenvironment, such as, chemokines and growth factors. Cell migration is central to development, wound repair and tissue remodeling, and plays a major role in cancer metastasis [1, 2]. Cell migration to specific sites of inflammation or infection is also essential for immune system function, with respect to the elimination of foreign or infectious agents [3]. Given the relevance of cell migration in a variety of physiological and pathological conditions, we attempted to identify novel genes that regulate cell migration using the short hairpin RNA (shRNA)-based functional selection of cell migration phenotypes. Lentivirally delivered shRNAs were used to produce stable transcript knockdown in mouse fibroblast cells and to conduct loss of function genetic selections.

Genetic screening for genes that regulate cell migration and morphology has been previously performed in various invertebrate model organisms, such as, *Drosophila melanogaster* and *Caenorhabditis elegans* [4, 5]. The development of small interfering RNA (siRNA) and shRNA technology has also made it feasible to perform genetic screening in mammalian cells. siRNAs can be generated in organisms using shRNAs, consisting of a sequence of 21–29 nt, a short loop region, and the reverse complement of the 21–29 nt region [6]. shRNA libraries have been used to perform genetic screens in tissue culture cells for a variety of phenotypes [7]. Recent studies have analyzed the closures of scratches in cellular monolayers after growth factor stimulation, using siRNA library targeting kinase and phosphatase genes [8, 9]. siRNA-based screening was performed to identify regulators of multiple cell adhesion complex formation [10], and RNAi screening to identify inhibitors of cell migration using SKOV-3 cells (a highly motile ovarian carcinoma cell line) [11]. More recently, new regulators of morphology, cytoskeletal organization, and cell migration in human cells have been identified using genome-wide RNAi morphology screening data in *D. melanogaster* cells [12]. Pooled shRNAs were also used for the genome-wide screen of cell migration regulators [13], and in that study, barcode microarray analysis was used to identify enriched shRNAs.

Herein, we adopted a selection and sequencing strategy to identify both cell migration-accelerating and -impairing genes using a genome-wide pooled shRNA library. Selection was performed using Boyden chamber assays followed by the separation and enrichment of cells with increased or decreased motility. shRNAs were then retrieved from selected cells and directly identified by half-hairpin barcode sequencing. This selection process resulted in the identification of 91 positive or negative regulators of cell migration; 29 of which genes had not been previously reported as cell migration regulators by RNAi screening. A set of 10 shRNAs were chosen for further validation studies, and these revealed remarkable dependences on the phosphoinositide-3 kinase (PI3K)/phosphatase and tensin homologue (PTEN)/AKT signaling pathway for cell migration acceleration or impairment.

Results

Genome-wide functional selection of cell migration regulators

To identify novel cell migration-regulating genes, RNAi-based functional selection was performed. After introducing 63,996 pooled lentiviral mouse shRNAs targeting 21,332 genes into NIH3T3 mouse fibroblast cells, the shRNAs that accelerated or impaired baseline motility were selected using the transwell migration assay (Fig 1a). Pooled recombinant lentivirus expressing shRNAs was generated by transfecting HEK293T cells with *pHAGE-mir30-RFP*-shRNA (targeting the mouse genome) (Fig 1b), *pVSV-G*, *pTat*, *pPM2* and *pRev*. NIH3T3 fibroblast cells were infected with the 63,996 pooled lentiviral mouse shRNA library at an MOI of 1 [14, 15]. Two days after infection, shRNA-infected cells were selected with puromycin, placed into the upper compartment of a transwell unit, and allowed to migrate through the perforated membrane to the lower compartment. Cells that exhibited accelerated or impaired migration were isolated from lower or upper compartments after 5 or 24 hr of incubation, respectively; 5 and 24 hr were chosen as optimal incubation times for these purposes (Supplementary Fig 1). In fact, different cell types and assay conditions were used in the previous migration screens. These discrepancies in the experimental setups may determine the degree of agreement of the current results with published data (Supplementary Table 1). Cells with the desired phenotypes were enriched by repeating the procedure five times. After enrichment, genomic DNA was isolated, and shRNAs integrated into chromosomes were retrieved by PCR amplification, cloned, and sequenced. The determined sequences of half-hairpin barcode were used to identify the shRNAs. This selection method identified 91 shRNAs that accelerated or impaired migration (Tables 1 and 2). Sixty two of the 91 identified target genes have been previously associated with cell migration by RNAi screen [8-10, 13, 16] (Supplementary Tables 2 and 3). The remaining 29 target genes had not been previously identified as cell migration regulators by RNAi screen. To determine relationships between cell migration regulators, a signaling network was built by IPA analysis (Fig 2). This analysis revealed that the newly identified cell migration regulators were closely linked to various cell movement signaling components (Fig 2a). The 91 cell migration-regulating genes identified were mapped to several major biological functions by IPA analysis; these functions included, cell movement and morphology (41%), cellular assembly and organization (21%), cell-to-cell signaling (20%), and protein trafficking and molecular transport (18%) (Fig 2b). Functional sub-networks were also constructed based on the biological functions in which they participate (Supplementary Fig 2a-d). Sub-network topology indicated a close interaction between the newly identified cell migration regulators and various functional components. Direct or indirect protein-protein interactions were also found between the identified regulators and other cell migration signaling components (Supplementary Fig 2e). Several additional targets were identified, not found in the primary selection, which might be predicted to modulate cell migration through network inference; these include CTNNB1, CDK4, MYC, IRS4, EIF3F, KIF5C, etc. In addition, a partial cell migration network was constructed, based on signaling pathways initiated by growth factor/receptor tyrosine kinase, fibronectin/integrin, or chemotactic factor/GPCR (Supplementary Fig 2f). Many nodes in the network were candidate genes identified in the current selection. PI3K, PTEN, and AKT emerged as convergent points in multiple networks. This result was not surprising, because the PI3K/AKT axis is known to regulate cell migration under diverse

conditions. Additionally, subcellular localization and disease association of the cell migration-regulating genes were analyzed (Supplementary Fig 3 and Supplementary Tables 4 and 5). The majority of the genes were associated with cancer and neurological diseases.

Validation of selected cell migration regulators

Among the 91 shRNAs identified (Tables 1 and 2), 10 were selected for further investigation (Supplementary Table 6). These shRNAs were selected, because little or no evidence linked the corresponding target genes with the regulation of cell migration. shRNA-induced phenotypes were validated using siRNA-mediated knockdown. To avoid off-target effects, five siRNA duplexes were synthesized for each shRNA candidate identified. Targeting sequences of the siRNAs were distinct from those of the shRNA constructs. The wound-healing assay revealed that transfection with the siRNAs of 5 migration-accelerating shRNA candidates (*mtmr1*, *lats2*, *dock3*, *myo5a,* and *ptpn14*) (Fig 3a,b) or with the siRNAs of 5 migration-impairing shRNA candidates (*csnk2a2*, *arid4a*, *ppp3cc*, *irf4,* and *alk*) (Fig 3c,d) increased or decreased, respectively, the motility of NIH3T3 fibroblast cells as compared with control siRNA transfectant. The cell migration-regulating activities of these candidates were also examined using the transwell migration assay, and similar results were obtained (Fig 4a,b). In addition, the cell migration-regulating activities of these candidates were confirmed in L929 mouse fibroblast and mouse embryonic fibroblast (MEF) cells using the transwell migration assay, which indicated that the observed cell migration-regulating effects of the siRNAs were not limited to a single cell line (Fig 4c,d). siRNA-mediated knockdown of the 10 target genes mentioned above was confirmed by RT-PCR (Fig 3b and d), and >50% knockdown was achieved for all siRNAs tested. siRNA-mediated knockdown of the target genes was also confirmed at the protein levels by Western blot analysis (Supplementary Fig 4a-e). Furthermore, it should be noted that the cell migration-regulating properties of siRNAs in the wound-healing assay and transwell migration assay were not due to effects on cell proliferation, as determined by MTT assay (Supplementary Fig 4f-h). Validation experiments were extended to other hits identified in the selection and network-derived candidates. Additional 36 hits (20 migration-accelerating shRNAs and 16 migration-impairing shRNAs) and 4 network-derived candidates (*ctnnb1*, *cdk4*, *myc,* and *irs4*) were tested using pooled retroviral shRNAs (Supplementary Table 7, Supplementary Fig 5, and Supplementary Movie 1). As a result, 71.7% (33/46) of the hits showed cell-migration regulating activity consistent with the primary screen. Among the 4 network-derived candidates, *ctnnb1* and *cdk4* shRNAs promoted and inhibited cell migration, respectively, thereby demonstrating 50% validation for the network analysis.

Common roles of the PI3K/PTEN/AKT pathways

Network analysis of the cell migration regulators identified indicated that the PI3K/PTEN/AKT signaling pathway plays a central role (Fig 2 and Supplementary Fig 2). PI3K/PTEN/AKT signaling has been previously associated with cell migration. For example, PI3K/AKT has been reported to enhance actin remodeling and to generate membrane protrusions, and to induce cell migration and cell invasion via remodeling of the actin cytoskeleton [17]. PTEN is a lipid phosphatase that dephosphorylates the D3 position of phosphatidylinositol-3,4,5-trisphosphate (PIP3), a second messenger produced by PI3K and that activates AKT [18, 19]. PTEN is also known to antagonize the cell migration-promoting

activity of PI3K. To determine whether the PI3K/PTEN/AKT signaling pathway is involved in the accelerated or impaired migration induced by shRNAs, we first assessed AKT phosphorylation after knocking down *dock3*, *mtmr1*, *ptpn14*, *lats2*, and *myo5a*, and after overexpressing *alk* and *irf4*. A knockdown of *dock3*, *mtmr1*, *ptpn14*, or *myo5a*, but not of *lats2*, or the overexpression of *alk* or *irf4* induced the phosphorylation of AKT (Fig 5a-c). The overexpression of *alk* or *irf4* in transfectants was confirmed by Western blot analysis (Fig 5d). In addition, we used pharmacological inhibitors of PI3K or AKT to evaluate the role of PI3K/AKT signaling in the accelerated or impaired cell migration by shRNAs. siRNA-mediated knockdown was done to upregulate cell migration for cell migration-inhibiting genes, while cDNA overexpression was done to upregulate cell migration for cell migration-promoting genes. The accelerated cell migration observed after *mtmr1*, *dock3*, *myo5a*, or *ptpn14* (but not *lats2*) knockdown was significantly attenuated by AKT or PI3K inhibitors in the wound-healing (Fig 6a) and transwell assays (Fig 7a). Similarly, the accelerated cell migration observed for *alk* or *irf4* overexpression was also attenuated by these inhibitors in the wound-healing (Fig 6b) and transwell assays (Fig 7b). Taken together, these results indicate that the cell migration promoters (*csnk2a2*, *arid4a*, *irf4,* and *alk*) and the inhibitors (*mtmr1*, *dock3*, *myo5a,* and *ptpn14*) mediate their effects via the PI3K/AKT pathway. Furthermore, at the concentration used in the current study, the PI3K and AKT inhibitors effectively inhibited downstream signaling pathways and were without effects on cell viability (Supplementary Fig 6). In order to gain a better understanding of the role of PI3K/AKT signaling in cell migration following specific gene knockdown, *foxo1* and *p70s6k1* (downstream components of the AKT pathway) were investigated. The phosphorylation of FOXO1 and p70S6K1 was increased after knockdown of the migration-inhibiting genes *dock3*, *mtmr1*, *ptpn14*, and *myo5a* and after the upregulation of the migration-promoting genes (*alk* and *irf4*) (Supplementary Fig 7). These results support that activation of the PI3K/AKT pathway, and downstream events, such as, FOXO1 and p70S6K1 phosphorylation, appear to be critically required for diverse cell migration regulators identified by unbiased functional selection.

Unique role of p55γ regulatory subunit of PI3K

In the next set of experiments, the cell migration-promoting gene *alk* was subjected to further investigation. Many receptor tyrosine kinases transduce their signals via specific interactions with SH2 domain-containing proteins such as regulatory subunits of PI3K [20]. Therefore, we asked whether the receptor tyrosine kinase *alk* regulates PI3K pathway through interaction with regulatory subunits of PI3K. Although ALK physically interacted with both p85α and p55γ regulatory subunits of PI3K (Fig 8a,b), ALK overexpression enhanced phosphorylation of p55γ, but not p85α, subunit (Fig 8c). The ALK-induced phosphorylation of p55γ regulatory subunit of PI3K was accompanied by AKT phosphorylation (Fig 8c) and translocation to plasma membrane (Fig 8d). GFP-fused AKT-PH domain was used to demonstrate the membrane translocation of AKT [21]. The critical role of p55γ and its phosphorylation in AKT activation and subsequent cell migration was further evaluated by siRNA-mediated knockdown of *p55γ* (Fig 8e,f and Supplementary Fig 8) [22]. *p55γ* siRNAs decreased ALK-induced AKT phosphorylation and cell migration, further supporting the unique role of p55γ subunit of PI3K in the Alk-promoted cell migration. These results indicate that ALK promotes cell migration by specifically

interacting with p55γ subunit of PI3K, rather than more common p85 subunit (Supplementary Fig 9a).

Discussion

We utilized lentivirus-based shRNA libraries targeting the entire mouse genome to enable genome-wide loss-of-function analysis by stable gene knockdown. Broad application of this shRNA library has already been reported in numerous studies on the identification of human disease-related genes [23-28] and genes associated with other phenotypes of interest [29-33]. In the current study, we aimed to identify diverse cellular pathways whose knockdowns have positive or negative effects on cell migration phenotypes. Some of the cell migration-regulating genes identified in the present study have well-established links to cellular motility, which validates the selection approach used. We also identified a number of previously uncharacterized cell migration regulators not previously identified by RNAi screening. Importantly, several novel cell migration regulators that were investigated in more detail were found to show marked downstream signaling convergence on the PI3K/PTEN/AKT pathway, which emphasizes the central roles of this pathway in cell migration.

Although the RNAi-based functional screening of cell migration regulators has been previously conducted, our approach differs in several ways. First, we performed unbiased genome scale shRNA selection, rather than screening, because phenotype-driven selection processes reduce false positives, because cells with given phenotypes are separated and enriched several times. The selection method used in the present study is straightforward and cost-effective as compared with array-based RNAi screen. Second, we used cells of fibroblast origin, which have higher baseline motilities than epithelial cells, as this allowed us to select cell migration accelerators and impairers at the same time. In the event, the selection method used identified many migration-promoting and inhibiting genes not previously reported. Third, we used direct cloning and sequencing of half-hairpin barcodes, rather than microarray analysis, in order to identify selected shRNAs. This process enabled the unbiased and direct selection of genes contributing to a given phenotype, because microarray-based identification involves statistical evaluation and a degree of ambiguity. In this method, however, it was difficult to assess how representative the selected shRNAs are to the starting shRNA library.

Among the functionally diverse 91 hits identified in the primary screen, targets of 13 shRNAs were protein kinases and protein phosphatases. Our results support the validity of the selection methods used and emphasize the critical roles played by protein kinases and phosphatases in cell motility regulation. Some of these kinases and phosphatases were included in our initial validation list, which comprised five migration-accelerating shRNA candidates (*mtmr1*, *lats2*, *dock3*, *myo5a* and *ptpn14*) and five migration-impairing shRNA candidates (*csnk2a2*, *arid4a*, *ppp3cc*, *irf4* and *alk*). In later studies, we found that the actions of some of these cell migration regulators, namely, *mtmr1*, *dock3*, *myo5a*, *ptpn14*, *csnk2a2*, *alk*, *irf4*, and *arid4a* (but not *lats2* or *ppp3cc*), are strongly dependent on the PI3K/PTEN/AKT pathway (Supplementary Fig 9b). Additional validation studies of 36 hits showed 71.7% overall correlation between the results of primary screen and secondary test.

Several of the cell migration-regulating genes identified in this study have been previously associated with the PI3K/PTEN/AKT pathway. Casein kinase 2 (CK2 or *csnk2*) is a physiologically relevant PTEN kinase, and CK2-mediated phosphorylation inhibits PTEN function, which in turn increases PIP3 levels, and thus, AKT phosphorylation. The expression levels and activities of CK2 subunits have been reported to be increased 3–5 fold in many human cancer and tumor cell lines [34-36]. Protein tyrosine phosphatase nonreceptor type 14 (*ptpn14*) is frequently mutated in a variety of human cancers. However, the cell signaling pathways regulated by Ptpn14 remain largely unknown [37]. In the present study, protein-protein interaction between PTPN14 and PTEN was identified by IPA analysis (Supplementary Fig 2e), which suggests that PTPN14 regulates cell migration by modulating PTEN activity. The physiological role of myotubularin-related protein 1 (*mtmr1*) has not been clearly determined, although recent studies have shown *mtmr1* is a phosphatase, like myotubularin, and can dephosphorylate both PtdIns3P and PtdIns3,5P2 *in vitro* [38, 39], which suggests its possible involvement in the PI3K/PTEN/AKT pathway.

Some of the cell migration regulators identified in this study appear to act independently of the PI3K/PTEN/AKT pathway. *Ppp3cc*, also known as calcineurin A subunit, is a Ca2+- and calmodulin-dependent serine/threonine protein phosphatase. In a recent study, calcineurin was shown to promote tumor cell invasion via transcriptional factor NFAT in breast cancer metastasis [40]. *Lats2* is a serine/threonine protein kinase belonging to the tumor suppressor family, and has been reported to participate in p53 signaling [41], and to be implicated in cell cycle regulation, apoptosis, centrosome duplication, and genomic stability [42-44]. Furthermore, our findings suggest that both *ppp3cc* and *lats2* promote or inhibit cell migration, respectively, via a mechanism not involving the PI3K/PTEN/AKT pathway.

In the present study, the activations of FOXO1 and p70S6K1 were investigated as signaling events downstream of the PI3K/PTEN/AKT pathway to determine the mechanistic basis of impaired or accelerated cell migration following specific gene knockdown. Forkhead box O (FOXO) proteins, which include FOXO1, FOXO3, FOXO4, and FOXO6, regulate many cancer-related phenotypes by inhibiting nuclear transcription factors. In the previous studies, activation of AKT led to FOXO1 phosphorylation and nuclear exclusion [45]. Furthermore, the nuclear exclusion of FOXO1 abolishes its inhibitory effect on Runx2 activity, and therefore, enhances Runx2-mediated gene transcription and the subsequent migration/invasion of cancer cells [46]. In addition, the AKT-mediated phosphorylation of FOXO1 induces its degradation by proteasome [47, 48]. Consistent with previous findings, we found that the level of FOXO1 was reduced after phosphorylation (Supplementary Fig 7). In a previous study, mTORC1 and mTORC2 signaling pathways were found to be involved in cytoskeletal rearrangement and cell migration [49, 50]. In particular, the activations of mTORC1 and p70S6K1 were found to be essential for the migration and invasion of cancer and non-cancer cells via cytoskeletal rearrangement [49, 51]. In the present study, the phosphorylation of AKT, FOXO1, and p70S6K1 was found to be associated with increased cell migration, which supports the notion that FOXO1 and p70S6K1 are downstream signaling components of PI3K/PTEN/AKT.

The PI3K family is categorized into 3 classes (class I, II, and III) and various subclasses based on their structure, substrate specificity, and regulation. The class I PI3K is the best-

characterized subfamily present in all cell types. They consist of a p110 catalytic subunit (α, β, γ, or δ) and a regulatory subunit (p85α, p85β, p55α, p55γ, or p50 α) [52]. Regulatory subunits are required to recruit the p110 catalytic subunit to specific cellular locations, thereby regulating its catalytic activity. The different regulatory subunits associate with distinct receptor tyrosine kinases [53] and show the specificity in mediating different PI3K signaling pathways [54]. However, the mechanisms by which these regulatory subunits regulate specific signaling pathways are not fully understood. p55γ, also known as p55PIK, binds the catalytic subunits and modulates PI3K activity in a manner similar to p85α and p85β [54, 55]. Our data indicate that p55γ was critically involved in the receptor tyrosine kinase Alk-promoted PI3K/AKT activation and cell migration. In the previous reports, p55γ regulatory subunit of PI3K promoted cell cycle progression [56], DNA synthesis [57], proliferation and differentiation of leukemia cells [58], and tumor angiogenesis via regulation of NF-κB signaling or expression of VEGF-A [59]. Furthermore, the protein levels of p55γ increased in colorectal, gastric, and ovarian cancers [56, 59, 60]. PI3K also plays an important role in the multiple steps of neurite outgrowth during nerve growth factor-stimulated differentiation and in the brain development [61].

Anaplastic lymphoma kinase (ALK) was originally identified as an oncogene in human anaplastic large cell lymphoma and neuroblastoma [62]. ALK displays the classical structural features of a receptor tyrosine kinase. In the previous studies, ALK mediated several signal transduction pathways, including JAK/STAT, RAS/MAPK, PI3K and PLCγ, and modulated various cellular functions, such as proliferation, angiogenesis, metabolism, and migration [63, 64]. An important role of ALK in the development and function of the nervous system has also been reported [65]. Brain expression of ALK changed during mouse [66] or zebrafish [67] embryogenesis, consistent with our results. However, little is known about physiological functions of ALK and its cognate ligands in vertebrate. In this study, for the first time, we have identified the p55γ regulatory subunit of PI3K as a target molecule of ALK during mouse fibroblast cell migration (Supplementary Fig 9a). Physical interaction between ALK and p55γ, ALK-induced phosphorylation of p55γ, and p55γ knockdown studies supported these findings. NIH3T3 cells express three isoforms of AKT. When the involvement of AKT isoforms in the ALK-induced cell migration was examined by knockdown of individual isoforms of *akt* (*akt1*, *akt2*, and *akt3*), all three isoforms of AKT were found to play an important role in the ALK-induced migration (Supplementary Fig 10). Although the critical role of p55γ in the ALK/AKT-induced cell migration has been demonstrated in the current study, it does not necessarily indicate that all the migration-related signaling is mediated via ALK/AKT and p55γ. Also, the phosphorylation of the regulatory subunit p55γ should not be regarded as a definitive indication for increased migration, as the cell migration depends on the relevant downstream PI3K targets and additional regulators. Further studies need to be conducted to better assess the importance of p55γ in cell migration in general.

In summary, the selection method used in the present study allowed us to identify a large number of genes that modulated cell migration. Furthermore, many of the cell migration-regulating genes identified have not been previously associated with cell migration. Although the precise regulatory mechanisms responsible for the effects of these cell migration regulators will only be determined by additional studies, the candidate gene list

obtained by the current selection process provides an integrated view regarding cell migration.

Methods

Reagents and cells

Specific small-molecule inhibitors, such as, Akt inhibitor (1L6-hydroxymethyl-chiro-inositol-2-(R)-2-O-methyl-3-O-octadecyl-*sn*-glycerocarbon) and PI3K inhibitor (LY294002) were purchased from Calbiochem (La Jolla, CA). Puromycin and mitomycin C were purchased from Sigma-Aldrich (St Louis, MO). All other chemicals, unless otherwise stated, were obtained from Sigma-Aldrich. NIH3T3 mouse fibroblast cells, L929 mouse fibroblast cells, and HEK293T human embryonic kidney epithelial cells were maintained in Dulbecco's modified Eagle's media (DMEM) supplemented with 10% heat-inactivated fetal bovine serum (FBS) (Invitrogen, Carlsbad, CA), 100 U/ml penicillin and 100 μg/ml streptomycin (Gibco-BRL, Rockville, MD). Phoenix Ampho cells were cultured in DMEM containing 10% FBS (Lonza, Walkersville, MD), hygromycin B (300 μg/ml), and diphtheria toxin (1 μg/ml) at 37°C and 5% CO_2. Mouse embryonic fibroblast (MEF) cell cultures were prepared from 13.5-days-old embryos of ICR mice [68].

Lentivirus production and titration

A 63,996 pooled lentiviral shRNA library targeting 21,332 mouse genes was generated by the transient transfection of HEK293T cells with *pHAGE-mir30-RFP*-shRNA (targeting the mouse genome), *pVSV-G*, *pTat*, *pPM2*, and *pRev* using LipofectAMINE 2000 (Invitrogen), in accordance with the manufacturer's instructions. The mir30-based shRNA constructs have been previously described [14]. Cell-free supernatants were harvested 2–3 days after transfection and were subsequently used to transduce NIH3T3 cells in the presence of 8 μg/ml polybrene. After 24 hr, virus-containing supernatants were removed by centrifugation. To optimize conditions for viral infection and to monitor virus titers, NIH3T3 fibroblast cells (1×10^6 cells) were seeded onto 100-mm culture plates 18 hr before infection and then incubated with 1 ml of RFP-carrying lentiviral stock for 6–8 hr, in the presence of polybrene (8 μg/ml). Fresh DMEM/10% FBS (2 ml) containing polybrene (8 μg/ml) was then added to the culture and incubation was continued. After another 24 hr, cells were removed from plates, and infection efficiencies and viral titers were determined by observing red fluorescence protein (RFP) under a fluorescence microscope (Olympus BX50; Tokyo). The titer of the viral shRNA library was ~7.23×10^6 plaque-forming units/ml.

Selection of cell migration regulators using shRNA library

NIH3T3 fibroblast cells were seeded at the density of 1×10^6 cells/100-mm culture plate. Three plates of NIH3T3 cells were infected with the lentiviral shRNA library at multiplicity of infection (MOI) of 1 in the presence of polybrene (8 μg/ml) (45 × representation for each shRNA). Two days after infection, cells were puromycin (10 ng/ml)-selected for 7 days, detached, seeded onto transwell culture inserts (8-μm pore membrane; Millipore, Billerica, MA) in 24-well plates (~4×10^4 cells/transwell culture insert/well), and incubated at 37°C for either 5 or 24 hr. The 5 hr time point was used to select migration enhancers and 24 hr was used to identify inhibitors of migration. Upper and lower transwell chambers were filled

with media containing 0% or 10% FBS, respectively, in order to induce the directional movement of cells. Infected cells (~3×10^6 cells) were divided and placed onto 72 transwell culture inserts. Cells that did or did not migrate were collected by trypsinizing cells adherent to the lower or upper faces of transwell culture inserts, respectively, and then reseeded onto transwell culture inserts. Cells from 72 individual wells were then allowed to re-migrate five times for enrichment purposes. Selected cells from the 72 transwell culture inserts were then combined. In order to identity the shRNAs integrated into the combined cells, a small amount (50 ng) of genomic DNA separately isolated from migrating or non-migrating cells was subjected to PCR. shRNA segments were amplified using the primer set: forward primer *JH353F*, TAGTGAAGCCACAGATGTA; reverse primer *BC1R*, CCTCCCCTACCCGGTAGA [14]. The resulting PCR fragments (453 bp) were gel-purified, cloned, and sequenced [69] (Fig 1). All clones were sequenced. The sequences of 22–27 nt, corresponding to the half-hairpins of shRNAs, were used to identify shRNAs.

Validation of primary hits using retroviral shRNAs

Retroviral shRNAs were generated by transient transfection of Phoenix Ampho packaging cells with each shRNA using Lipofectamine 2000 in accordance with the manufacturer's instructions. Cell-free supernatants were harvested 2–3 days after transfection and subsequently were used to transduce NIH3T3 fibroblast cells in the presence of 8 μg/ml polybrene. To optimize conditions of viral infection and to monitor virus titer, a test construct of the retroviral vector carrying GFP (*pFB-hrGFP*) (Stratagene) was used. For infection of NIH3T3 fibroblast cells, cells (1×10^5 cells/well) were seeded onto 60-mm culture plates 18 hr before infection and incubated with 1 ml of virus stock for 6–8 hr in the presence of polybrene (8 μg/ml). Then, 2 ml of fresh DMEM/10% FBS containing polybrene (8 μg/ml) was added to the culture and the incubation was continued. After another 24 hr, cells were removed from the plates, and infection efficiency and viral titer were determined by the count of GFP-positive cells using FACS. NIH3T3 fibroblast cells were infected with the retroviral shRNA at MOI of 1–3. For high-throughput screening, Essen Incucyte™ and Woundmaker™ (Essen BioScience, Inc., Ann Arbor, MI) were used. In brief, the cell migration algorithm analyzed each image and assigned a well-specific wound mask that corresponded to the initial scratch wound. Scratch wound mask followed migrating cells as they moved into the initial wound, creating a measurement of relative wound density or wound closure.

Pathway and network analyses

The accession numbers of identified DNAs were exported to Ingenuity Pathway Analysis (IPA, Ingenuity Systems) for network analysis. The statistical significance of each network or list was determined by IPA using Fisher's Exact test ($p < 0.05$). IPA was also used to construct networks of protein-protein and other regulatory interactions. For pathway construction, the IPA database used currently available knowledge on genes, proteins, chemicals, normal and disease cellular processes, signaling, and cellular functions.

Transient transfection with siRNA or cDNA

Desalted and preannealed siRNA duplexes were purchased from Genolution Pharmaceuticals (Seoul, Korea). The siRNAs were designed using a proprietary algorithm

devised by Genolution Pharmaceuticals. Sequence information for the siRNAs used for validation is given in Supplementary Table 6. To knockdown specific gene expression, NIH3T3 mouse fibroblast cells were transfected with siRNAs at a final concentration of 10 nM using LipofectAMINE (Invitrogen), according to the manufacturer's instructions. Cells were harvested 24–48 hr after transfection, and the potencies of siRNAs to silence gene expression were measured by RT-PCR or Western blot analysis. A control random sequence siRNA was also purchased from Genolution Pharmaceuticals and used as negative control. The full-length cDNAs of mouse *alk* or *irf4* were cloned into the expression vectors *pcDNA3* or *pFlag*, respectively. NIH3T3 fibroblast cells in six-well plates were transiently transfected with 3 μg of *alk* or *irf4* cDNA using LipofectAMINE. The empty vector *pcDNA3* or *pFlag* was used as control for the transient expression of *alk* or *irf4*. One or two days after transfection, cells were used for experiments. The expressions of *alk* and *irf4* mRNAs and proteins in transient transfectants were confirmed by RT-PCR or Western blot analysis, respectively.

Reverse transcription-PCR

Total RNA was extracted from NIH3T3 cells in 6-well plates using TRIzol reagent (Invitrogen), according to the manufacturer's instructions. Reverse transcription was conducted using Superscript II (Invitrogen) and oligo(dT) primer. PCR amplification, using specific primer sets, was carried out at an annealing temperature of 55–60°C for 20–30 cycles. PCR was performed by using a DNA Engine Tetrad Peltier Thermal Cycler (MJ Research, Waltham, MA). To analyze PCR products, 10 μl of each PCR reaction product was electrophoresed on 1% agarose gel followed by ethidium bromide staining and detection under UV light. *β-actin* was used as internal control. The nucleotide sequences of the primers used were based on published cDNA sequences (Supplementary Table 8).

Wound-healing assay

For the *in vitro* wound healing assay, a scratch was created by using a 10 μl pipette tip on confluent cell monolayers in 24-well culture plates, and then DMEM containing 10% FBS, 100 U/ml penicillin, and 100 μg/ml streptomycin was added. Cells were then incubated at 37°C under 5% CO_2 to enable migration into wounds, which were then observed under a light microscope (Olympus CK2; X100). In order to rule out confounding effect of cell proliferation, cells were treated with the mitosis inhibitor mitomycin-C at a final concentration of 10 μg/ml for 2 hr before wounding. Relative cell migration distances were calculated by subtracting final wound widths from initial values [70]. Three non-overlapping fields were selected and examined per well (three wells per experimental group). The results are presented as fold increases in migration distance versus control condition.

Three-dimensional cell migration assay

Cell migration was also measured using transwell culture inserts (8-μm pore membrane; Millipore), according to the manufacturer's instructions. In brief, cells were transfected with the siRNAs of migration accelerating or impairing genes. At 24 hr after transfection, cells were harvested by trypsinization, resuspended in DMEM, and added to upper wells at 4×10^4 cells/well. Growth media were placed into base wells, which were separated from top wells by a polycarbonate filter membrane. Cells were incubated at 37°C for 6 hr (for

accelerating siRNAs) or 9 hr (for impairing siRNAs). Non-migrating cells on the inner sides of transwell culture inserts were then removed with a cotton swab, and migrated cells on the undersides of inserts were fixed with methanol for 10 min and stained with Mayer's hematoxylin (DakoCytomation, Glostrup, Denmark) for 20 min. Photomicrographs of 5 random fields were taken (Olympus CK2; X100), and cells were then counted using a NIH image J program (NIH Image; Bethesda, MD). In brief, images were binary thresholded at 50% of the background level, and particles were then converted to a sub-threshold image area with a size larger than 200 pixels, which was determined to be sufficient to identify migrated cells. Numbers of cells were counted and results were analyzed statistically.

Western blot analysis

Cells were lysed in triple-detergent lysis buffer (50 mM Tris-HCl, pH 8.0, 150 mM NaCl, 0.02% sodium azide, 0.1% SDS, 1% NP-40, 0.5% sodium deoxycholate, and 1 mM phenylmethylsulfonyl fluoride). Protein concentrations in cell lysates were determined using the Bio-Rad protein assay kit (Bio-Rad, Hercules, CA). Equal amounts of protein were separated by 8 or 12% SDS-PAGE and transferred to Hybond ECL nitrocellulose membranes (Amersham Biosciences, Piscataway, NJ). Membranes were blocked with 5% skim milk and sequentially incubated with primary antibodies [rabbit polyclonal anti-phospho-PI3 kinase p85α (Tyr458)/p55γ (Tyr199) antibody (1:500 dilution; Cell Signaling Technology, Danvers, MA); rabbit polyclonal anti-PI3 kinase p85α antibody (1:1,000 dilution; Cell Signaling Technology); goat polyclonal anti-p55γ antibody (1:500 dilution; Santa Cruz, Santa Cruz, CA); rabbit polyclonal anti-phospho-AKT (Ser473) antibody (1:1,000 dilution; Cell Signaling Technology); rabbit polyclonal anti-AKT antibody (1:1,000 dilution; Cell Signaling Technology); rabbit polyclonal anti-phospho-FOXO1 (Ser256) antibody (1:500 dilution; Cell Signaling Technology); rabbit polyclonal anti-FOXO1 antibody (1:500 dilution; Cell Signaling Technology); rabbit polyclonal anti-phospho-p70S6 kinase (Thr389) antibody (1:1,000 dilution; Cell Signaling Technology); rabbit polyclonal anti-p70S6 kinase antibody (1:1,000 dilution; Cell signaling Technology); monoclonal anti-α-tubulin antibody (1:2,000 dilution; Sigma-Aldrich); rabbit polyclonal anti-MTMR1 antibody (1:500 dilution; Sigma-Aldrich); goat polyclonal anti-PTPN14 antibody (1:500 dilution; Santa Cruz); rabbit polyclonal anti-DOCK3 antibody (1:500 dilution; Abcam, Cambridge, MA); rabbit polyclonal anti-IRF4 antibody (1:500 dilution; Cell Signaling Technology); rabbit polyclonal anti-ALK antibody (1:500 dilution; Novus Biologicals, Littleton, CO)], and HRP-conjugated secondary antibodies (1:10,000 dilution; anti-rabbit-, anti-mouse-, or anti-goat-IgG antibody; Amersham Biosciences), and then detected using an ECL detection kit (Amersham Biosciences).

Assessment of cell proliferation and viability by MTT assay

NIH3T3 cells in 96-well culture plates were transfected with siRNAs or cDNA constructs and incubated for 24 – 72 hr. At each designated time point after transfection, culture media were removed, MTT (3-[4,5-dimethylthiazol-2-yl]-2,5-diphenyltetrazolium bromide) (0.5 mg/ml) was added, and cells were incubated at 37°C for 2 hr in a CO_2 incubator. After dissolving the insoluble crystals that formed in DMSO, absorbance was measured at 570 nm using a microplate reader (Anthos Labtec Instruments, Wals, Austria).

Statistical analysis

Results are presented as the means ± SDs of three or more independent experiments, unless stated otherwise. The one-way ANOVA with Dunnett's multiple-comparison test was used to compare treatments. SPSS version 18.0K (SPSS Inc., Chicago, IL) was used for the analysis, and p value differences of < 0.05 were considered statistically significant.

Supplementary Material

Refer to Web version on PubMed Central for supplementary material.

Acknowledgements

This work was supported by the National Research Foundation of Korea (NRF) grant funded by the Korea government (MSIP) (No. 2008–0062282), and by a grant from the Korean Health technology R&D Project, Ministry of Health & Welfare, Republic of Korea (A111345). This work was also supported by a DOD Breast Cancer Innovator Award and a grant from SU2C to S.J.E. at the Howard Hughes Medical Institute.

Abbreviations

shRNA	small hairpin RNA
IPA	ingenuity pathway analysis
DAVID	database for annotation, visualization and integrated discovery
PI3K	phosphoinositide-3-kinase
PTEN	phosphatase and tensin homolog
FOXO1	Forkhead box protein O1
ALK	anaplastic lymphoma kinase
MEF	mouse embryonic fibroblast

References

1. Vicente-Manzanares M, Webb DJ, Horwitz AR. Cell migration at a glance. J Cell Sci 118, 4917–4919 (2005). [PubMed: 16254237]
2. Franz CM, Jones GE, Ridley AJ. Cell migration in development and disease. Dev Cell 2, 153–158 (2002). [PubMed: 11832241]
3. Luster AD, Alon R, von Andrian UH. Immune cell migration in inflammation: present and future therapeutic targets. Nat Immunol 6, 1182–1190 (2005). [PubMed: 16369557]
4. Cram EJ, Shang H, Schwarzbauer JE. A systematic RNA interference screen reveals a cell migration gene network in C. elegans. J Cell Sci 119, 4811–4818 (2006). [PubMed: 17090602]
5. Wang X, et al. Analysis of cell migration using whole-genome expression profiling of migratory cells in the Drosophila ovary. Dev Cell 10, 483–495 (2006). [PubMed: 16580993]
6. Dykxhoorn DM, Novina CD, Sharp PA. Killing the messenger: short RNAs that silence gene expression. Nat Rev Mol Cell Biol 4, 457–467 (2003). [PubMed: 12778125]
7. Paddison PJ, et al. A resource for large-scale RNA-interference-based screens in mammals. Nature 428, 427–431 (2004). [PubMed: 15042091]
8. Simpson KJ, et al. Identification of genes that regulate epithelial cell migration using an siRNA screening approach. Nat Cell Biol 10, 1027–1038 (2008). [PubMed: 19160483]

9. Vitorino P, Meyer T. Modular control of endothelial sheet migration. Genes Dev 22, 3268–3281 (2008). [PubMed: 19056882]
10. Winograd-Katz SE, Itzkovitz S, Kam Z, Geiger B. Multiparametric analysis of focal adhesion formation by RNAi-mediated gene knockdown. J Cell Biol 186, 423–436 (2009). [PubMed: 19667130]
11. Collins CS, et al. A small interfering RNA screen for modulators of tumor cell motility identifies MAP4K4 as a promigratory kinase. Proc Natl Acad Sci U S A 103, 3775–3780 (2006). [PubMed: 16537454]
12. Bai SW, et al. Identification and characterization of a set of conserved and new regulators of cytoskeletal organization, cell morphology and migration. BMC Biol 9, 54 (2011). [PubMed: 21834987]
13. Smolen GA, et al. A genome-wide RNAi screen identifies multiple RSK-dependent regulators of cell migration. Genes Dev 24, 2654–2665 (2010). [PubMed: 21062900]
14. Schlabach MR, et al. Cancer proliferation gene discovery through functional genomics. Science 319, 620–624 (2008). [PubMed: 18239126]
15. Silva JM, et al. Second-generation shRNA libraries covering the mouse and human genomes. Nat Genet 37, 1281–1288 (2005). [PubMed: 16200065]
16. Yang J, et al. Genome-wide RNAi screening identifies genes inhibiting the migration of glioblastoma cells. PLoS ONE 8, e61915 (2013). [PubMed: 23593504]
17. Qian Y, et al. PI3K induced actin filament remodeling through Akt and p70S6K1: implication of essential role in cell migration. Am J Physiol Cell Physiol 286, C153–163 (2004). [PubMed: 12967912]
18. Song MS, Salmena L, Pandolfi PP. The functions and regulation of the PTEN tumour suppressor. Nat Rev Mol Cell Biol 13, 283–296 (2012). [PubMed: 22473468]
19. Martelli AM, et al. Targeting the translational apparatus to improve leukemia therapy: roles of the PI3K/PTEN/Akt/mTOR pathway. Leukemia 25, 1064–1079 (2011). [PubMed: 21436840]
20. Schlessinger J, Ullrich A. Growth factor signaling by receptor tyrosine kinases. Neuron 9, 383–391 (1992). [PubMed: 1326293]
21. Raucher D, et al. Phosphatidylinositol 4,5-bisphosphate functions as a second messenger that regulates cytoskeleton-plasma membrane adhesion. Cell 100, 221–228 (2000). [PubMed: 10660045]
22. Zhu Q, et al. Phosphoinositide 3-OH kinase p85alpha and p110beta are essential for androgen receptor transactivation and tumor progression in prostate cancers. Oncogene 27, 4569–4579 (2008). [PubMed: 18372911]
23. Kim DH, Rossi JJ. Strategies for silencing human disease using RNA interference. Nat Rev Genet 8, 173–184 (2007). [PubMed: 17304245]
24. Cheng JC, Moore TB, Sakamoto KM. RNA interference and human disease. Mol Genet Metab 80, 121–128 (2003). [PubMed: 14567961]
25. Alvarez-Calderon F, Gregory MA, Degregori J. Using functional genomics to overcome therapeutic resistance in hematological malignancies. Immunol Res 33, 100–115 (2012).
26. Dahlman KB, et al. Modulators of prostate cancer cell proliferation and viability identified by short-hairpin RNA library screening. PLoS ONE 7, e34414 (2012). [PubMed: 22509301]
27. Hu K, Law JH, Fotovati A, Dunn SE. Small interfering RNA library screen identified polo-like kinase-1 (PLK1) as a potential therapeutic target for breast cancer that uniquely eliminates tumor-initiating cells. Breast Cancer Res 14, R22 (2012). [PubMed: 22309939]
28. Wan X, et al. Identification of the FoxM1/Bub1b signaling pathway as a required component for growth and survival of rhabdomyosarcoma. Cancer Res 72, 5889–5899 (2012). [PubMed: 23002205]
29. Draviam VM, et al. A functional genomic screen identifies a role for TAO1 kinase in spindle-checkpoint signalling. Nat Cell Biol 9, 556–564 (2007). [PubMed: 17417629]
30. Root DE, Hacohen N, Hahn WC, Lander ES, Sabatini DM. Genome-scale loss-of-function screening with a lentiviral RNAi library. Nat Methods 3, 715–719 (2006). [PubMed: 16929317]

31. Hu G, Kim J, Xu Q, Leng Y, Orkin SH, Elledge SJ. A genome-wide RNAi screen identifies a new transcriptional module required for self-renewal. Genes Dev 23, 837–848 (2009). [PubMed: 19339689]
32. Schmitz MH, et al. Live-cell imaging RNAi screen identifies PP2A-B55alpha and importin-beta1 as key mitotic exit regulators in human cells. Nat Cell Biol 12, 886–893 (2010). [PubMed: 20711181]
33. Yang R, et al. A genome-wide siRNA screen to identify modulators of insulin sensitivity and gluconeogenesis. PLoS ONE 7, e36384 (2012). [PubMed: 22590537]
34. Romieu-Mourez R, Landesman-Bollag E, Seldin DC, Sonenshein GE. Protein kinase CK2 promotes aberrant activation of nuclear factor-kappaB, transformed phenotype, and survival of breast cancer cells. Cancer Res 62, 6770–6778 (2002). [PubMed: 12438279]
35. Channavajhala P, Seldin DC. Functional interaction of protein kinase CK2 and c-Myc in lymphomagenesis. Oncogene 21, 5280–5288 (2002). [PubMed: 12149649]
36. Munstermann U, Fritz G, Seitz G, Lu YP, Schneider HR, Issinger OG. Casein kinase II is elevated in solid human tumours and rapidly proliferating non-neoplastic tissue. Eur J Biochem 189, 251–257 (1990). [PubMed: 2159876]
37. Zhang P, et al. Identification and functional characterization of p130Cas as a substrate of protein tyrosine phosphatase nonreceptor 14. Oncogene 32, 2087–2095 (2012). [PubMed: 22710723]
38. Buj-Bello A, et al. Muscle-specific alternative splicing of myotubularin-related 1 gene is impaired in DM1 muscle cells. Hum Mol Genet 11, 2297–2307 (2002). [PubMed: 12217958]
39. Tronchere H, et al. Production of phosphatidylinositol 5-phosphate by the phosphoinositide 3-phosphatase myotubularin in mammalian cells. J Biol Chem 279, 7304–7312 (2004). [PubMed: 14660569]
40. Ryeom S, et al. Targeted deletion of the calcineurin inhibitor DSCR1 suppresses tumor growth. Cancer Cell 13, 420–431 (2008). [PubMed: 18455125]
41. Aylon Y, Michael D, Shmueli A, Yabuta N, Nojima H, Oren M. A positive feedback loop between the p53 and Lats2 tumor suppressors prevents tetraploidization. Genes Dev 20, 2687–2700 (2006). [PubMed: 17015431]
42. McPherson JP, et al. Lats2/Kpm is required for embryonic development, proliferation control and genomic integrity. EMBO J 23, 3677–3688 (2004). [PubMed: 15343267]
43. Ke H, et al. Putative tumor suppressor Lats2 induces apoptosis through downregulation of Bcl-2 and Bcl-x(L). Exp Cell Res 298, 329–338 (2004). [PubMed: 15265683]
44. Li Y, Pei J, Xia H, Ke H, Wang H, Tao W. Lats2, a putative tumor suppressor, inhibits G1/S transition. Oncogene 22, 4398–4405 (2003). [PubMed: 12853976]
45. Huang H, Tindall DJ. Dynamic FoxO transcription factors. J Cell Sci 120, 2479–2487 (2007). [PubMed: 17646672]
46. Zhang H, et al. FOXO1 inhibits Runx2 transcriptional activity and prostate cancer cell migration and invasion. Cancer Res 71, 3257–3267 (2011). [PubMed: 21505104]
47. Huang H, Tindall DJ. Regulation of FOXO protein stability via ubiquitination and proteasome degradation. Biochim Biophys Acta 1813, 1961–1964 (2011). [PubMed: 21238503]
48. Brunet A, et al. Akt promotes cell survival by phosphorylating and inhibiting a Forkhead transcription factor. Cell 96, 857–868 (1999). [PubMed: 10102273]
49. Meng Q, Xia C, Fang J, Rojanasakul Y, Jiang BH. Role of PI3K and AKT specific isoforms in ovarian cancer cell migration, invasion and proliferation through the p70S6K1 pathway. Cell Signal 18, 2262–2271 (2006). [PubMed: 16839745]
50. Liu L, Li F, Cardelli JA, Martin KA, Blenis J, Huang S. Rapamycin inhibits cell motility by suppression of mTOR-mediated S6K1 and 4E-BP1 pathways. Oncogene 25, 7029–7040 (2006). [PubMed: 16715128]
51. Poon M, Marx SO, Gallo R, Badimon JJ, Taubman MB, Marks AR. Rapamycin inhibits vascular smooth muscle cell migration. J Clin Invest 98, 2277–2283 (1996). [PubMed: 8941644]
52. Bunney TD, Katan M. Phosphoinositide signalling in cancer: beyond PI3K and PTEN. Nat Rev Cancer 10, 342–352 (2010). [PubMed: 20414202]

53. Inukai K, et al. Five isoforms of the phosphatidylinositol 3-kinase regulatory subunit exhibit different associations with receptor tyrosine kinases and their tyrosine phosphorylations. FEBS Lett 490, 32–38 (2001). [PubMed: 11172806]
54. Vanhaesebroeck B, Guillermet-Guibert J, Graupera M, Bilanges B. The emerging mechanisms of isoform-specific PI3K signalling. Nat Rev Mol Cell Biol 11, 329–341 (2010). [PubMed: 20379207]
55. Courtney KD, Corcoran RB, Engelman JA. The PI3K pathway as drug target in human cancer. J Clin Oncol 28, 1075–1083 (2010). [PubMed: 20085938]
56. Hu J, et al. Overexpression of the N-terminal end of the p55gamma regulatory subunit of phosphatidylinositol 3-kinase blocks cell cycle progression in gastric carcinoma cells. Int J Oncol 26, 1321–1327 (2005). [PubMed: 15809724]
57. Wang G, et al. PI3K Stimulates DNA Synthesis and Cell-Cycle Progression via Its p55PIK Regulatory Subunit Interaction with PCNA. Mol Cancer Ther 12, 2100–2109 (2013). [PubMed: 23939377]
58. Wang G, et al. Blocking p55PIK signaling inhibits proliferation and induces differentiation of leukemia cells. Cell Death Differ 19, 1870–1879 (2012). [PubMed: 22722333]
59. Wang G, et al. p55PIK-PI3K stimulates angiogenesis in colorectal cancer cell by activating NF-kappaB pathway. Angiogenesis 16, 561–573 (2013). [PubMed: 23354733]
60. Zhang L, et al. Integrative genomic analysis of phosphatidylinositol 3'-kinase family identifies PIK3R3 as a potential therapeutic target in epithelial ovarian cancer. Clin Cancer Res 13, 5314–5321 (2007). [PubMed: 17875760]
61. Waite K, Eickholt BJ. The neurodevelopmental implications of PI3K signaling. Curr Top Microbiol Immunol 346, 245–265 (2010). [PubMed: 20582530]
62. Roskoski R Jr. Anaplastic lymphoma kinase (ALK): structure, oncogenic activation, and pharmacological inhibition. Pharmacol Res 68, 68–94 (2013). [PubMed: 23201355]
63. Polgar D, et al. Truncated ALK derived from chromosomal translocation t(2;5)(p23;q35) binds to the SH3 domain of p85-PI3K. Mutat Res 570, 9–15 (2005). [PubMed: 15680399]
64. Wasik MA, Zhang Q, Marzec M, Kasprzycka M, Wang HY, Liu X. Anaplastic lymphoma kinase (ALK)-induced malignancies: novel mechanisms of cell transformation and potential therapeutic approaches. Semin Oncol 36, S27–35 (2009). [PubMed: 19393833]
65. Palmer RH, Vernersson E, Grabbe C, Hallberg B. Anaplastic lymphoma kinase: signalling in development and disease. Biochem J 420, 345–361 (2009). [PubMed: 19459784]
66. Iwahara T, et al. Molecular characterization of ALK, a receptor tyrosine kinase expressed specifically in the nervous system. Oncogene 14, 439–449 (1997). [PubMed: 9053841]
67. Yao S, Cheng M, Zhang Q, Wasik M, Kelsh R, Winkler C. Anaplastic lymphoma kinase is required for neurogenesis in the developing central nervous system of zebrafish. PLoS ONE 8, e63757 (2013). [PubMed: 23667670]
68. Serrano M, Lin AW, McCurrach ME, Beach D, Lowe SW. Oncogenic ras provokes premature cell senescence associated with accumulation of p53 and p16INK4a. Cell 88, 593–602 (1997). [PubMed: 9054499]
69. Seo M, Lee WH, Suk K. Identification of novel cell migration-promoting genes by a functional genetic screen. FASEB J 24, 464–478 (2010). [PubMed: 19812375]
70. Bassi R, et al. HMGB1 as an autocrine stimulus in human T98G glioblastoma cells: role in cell growth and migration. J Neurooncol 87, 23–33 (2008). [PubMed: 17975708]

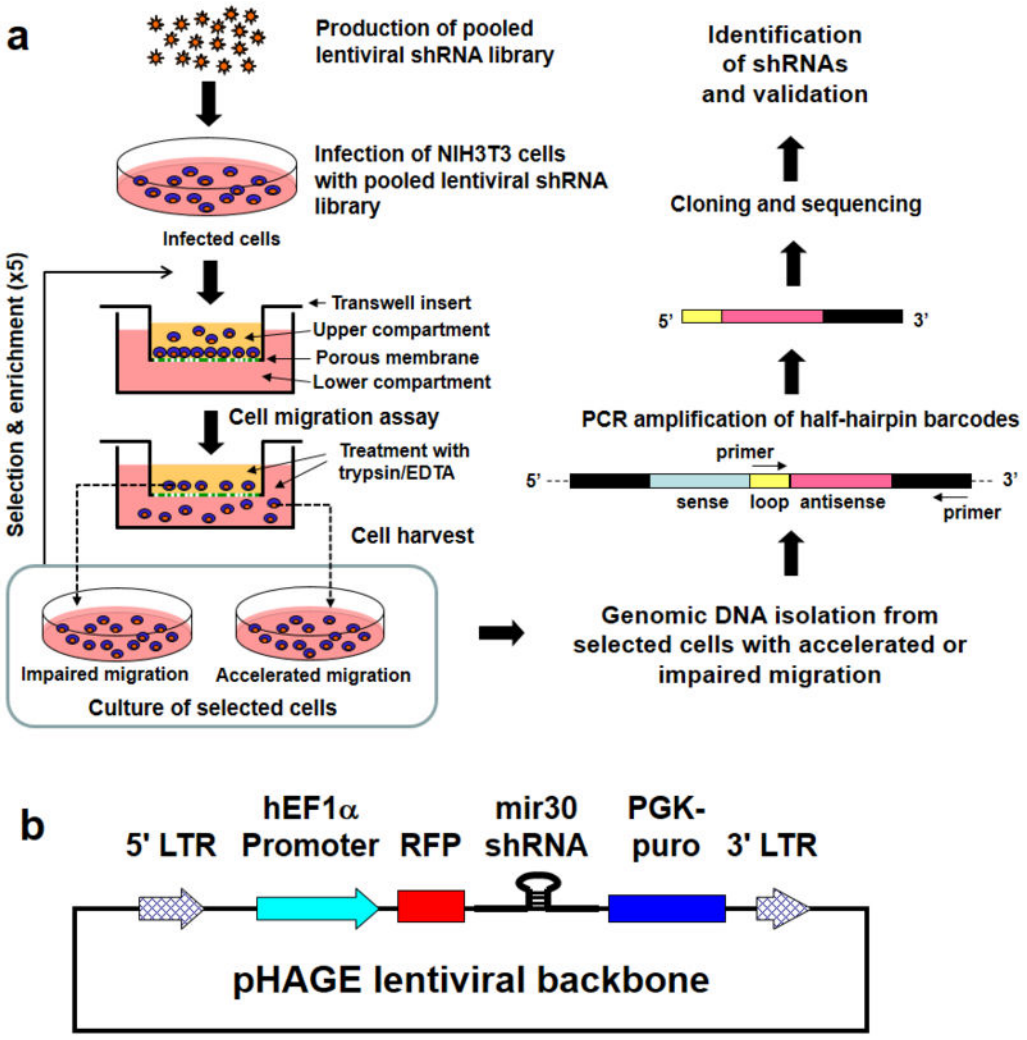

Figure 1. Schematic representation of the RNAi-based selection of cell migration regulators.

(**a**) Overview of the selection procedure. The production and infection of genome-wide lentiviral shRNA library are described in Methods. Two days after lentiviral infection, NIH3T3 mouse fibroblast cells were seeded onto transwell inserts and allowed to migrate across the porous membrane at 37°C for 5 or 24 hr, to select cells with an increased or decreased migration phenotype, respectively. Migrated or non-migrated cells were collected by trypsin-EDTA treatment from the lower or upper faces, respectively, of inserts, and reseeded onto transwell culture inserts for a second round of selection (this process was repeated five times). After the final round of selection, shRNAs were retrieved by PCR from selected cells and identified by sequencing. (**b**) Diagram of *pHAGE-mir30-RFP*-shRNA vector. The pooled lentiviral vector contained 63,996 different mir30-based shRNAs targeting 21,332 mouse genes.

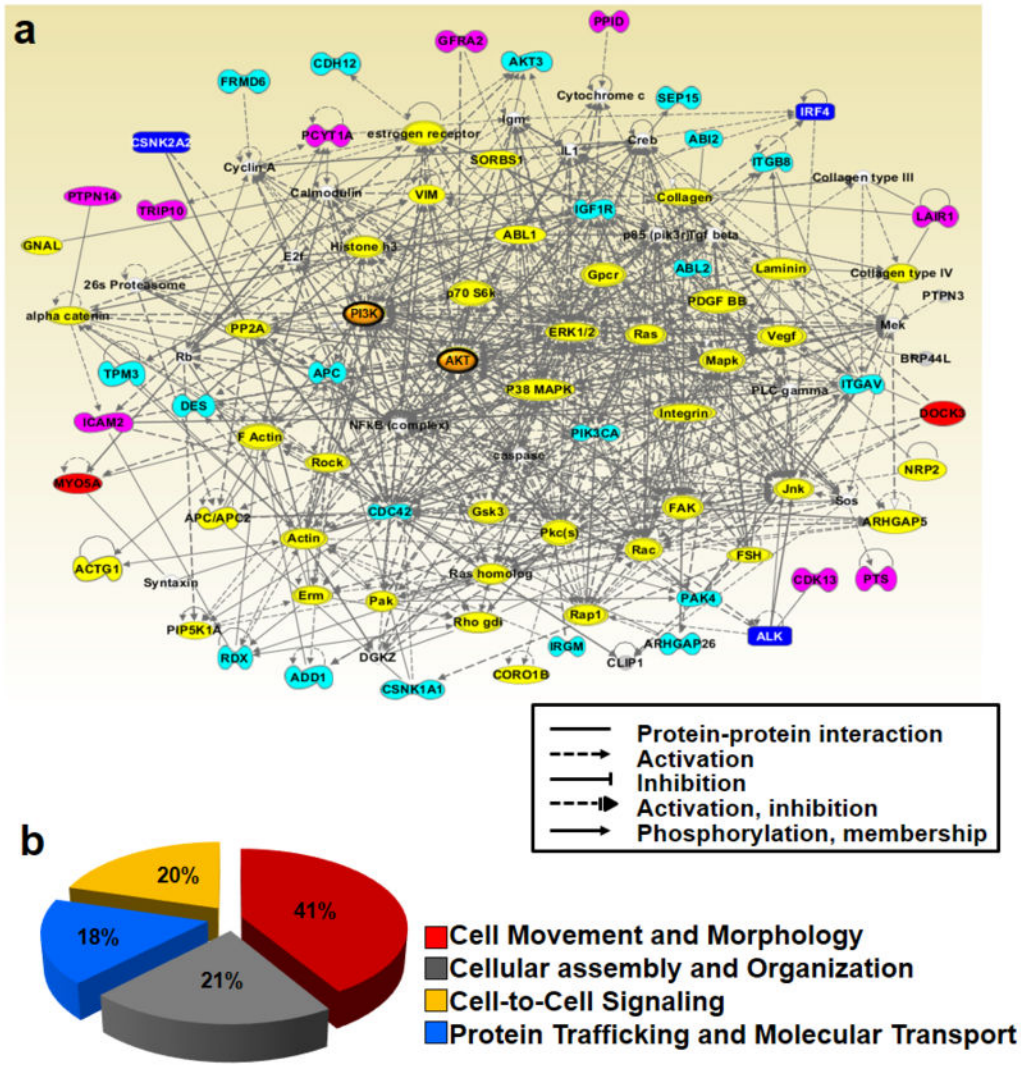

Figure 2. Construction of the signaling network of cell migration regulators and their classification based on biological functions.

(**a**) A relevant signaling network was constructed from the 91 cell migration-regulating genes identified by Ingenuity Pathway Analysis (IPA). Newly identified cell migration regulators were linked to various previously reported cell movement signaling components (yellow). Green, cell migration–accelerating genes; blue, cell migration–accelerating genes validated by siRNA; pink, cell migration-impairing genes; red, cell migration–impairing genes validated by siRNA study. PI3K and AKT are highlighted in brown. (**b**) The biological functions of cell migration regulators were categorized by IPA analysis, which showed; 41% were cell movement and morphology related, 21% were cellular assembly and organization related, 20% were cell-to-cell signaling related, and 18% were protein trafficking and molecular transport related.

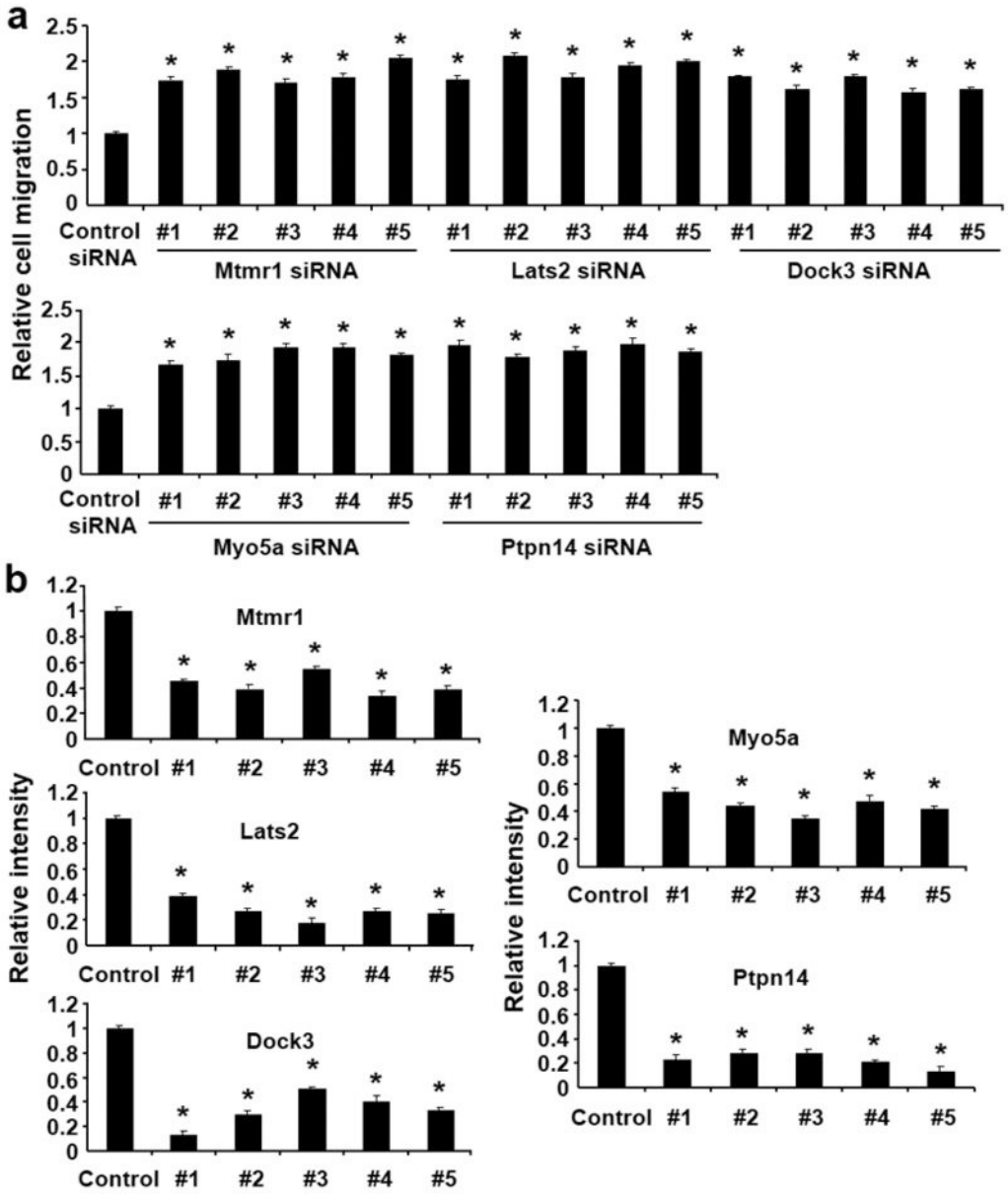

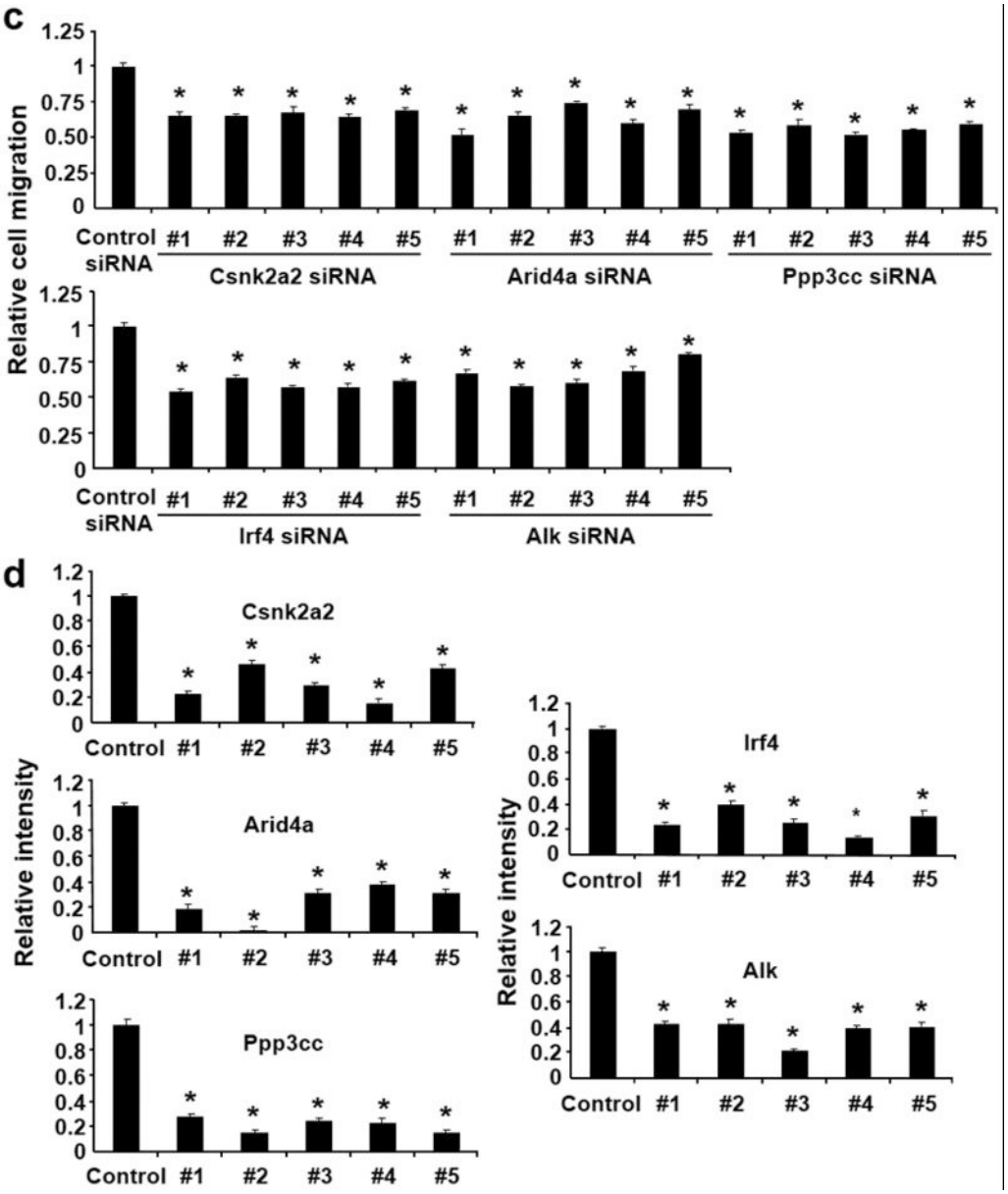

Figure 3. Validation of the gene targets found by the RNAi-based functional selection.

(**a**) NIH3T3 fibroblast cells were transiently transfected with control siRNA or one of five siRNAs (#1 to #5) targeting *mtmr1*, *lats2*, *dock3*, *myo5a*, or *ptpn14*. At 24 hr after transfection, wound-healing assays were performed to evaluate cell migration. (**b**) Efficiencies of siRNA-mediated target gene knockdown were confirmed by RT-PCR followed by densitometric analysis. (**c**) NIH3T3 cells were transiently transfected with control siRNA or one of five siRNAs (#1 to #5) for each target gene identified (*csnk2a2*, *arid4a*, *ppp3cc*, *irf4*, and *alk*). After 24 hr, wound-healing assays were performed to evaluate cell migration. Cell migration was quantified by measuring degrees of wound closure, as described in Methods. The results shown are means ± SDs ($n = 3$). *$p < 0.05$ represents significantly different from control siRNA-transfected cells. (**d**) Efficiencies of siRNA-mediated target gene knockdown were confirmed by RT-PCR and densitometric analysis. β-

actin was used as the internal control. The results are means ± SDs ($n = 3$); * p values of < 0.05 indicate significantly different from control siRNA-transfected cells.

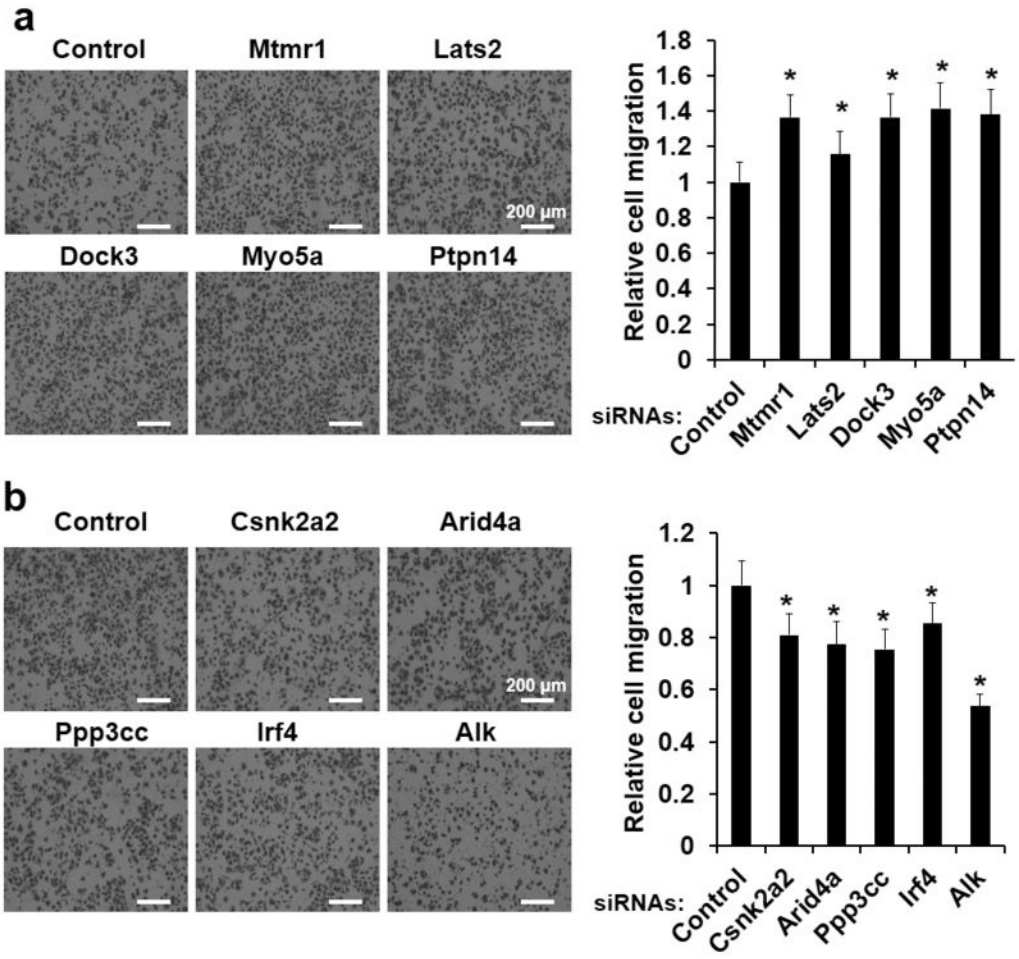

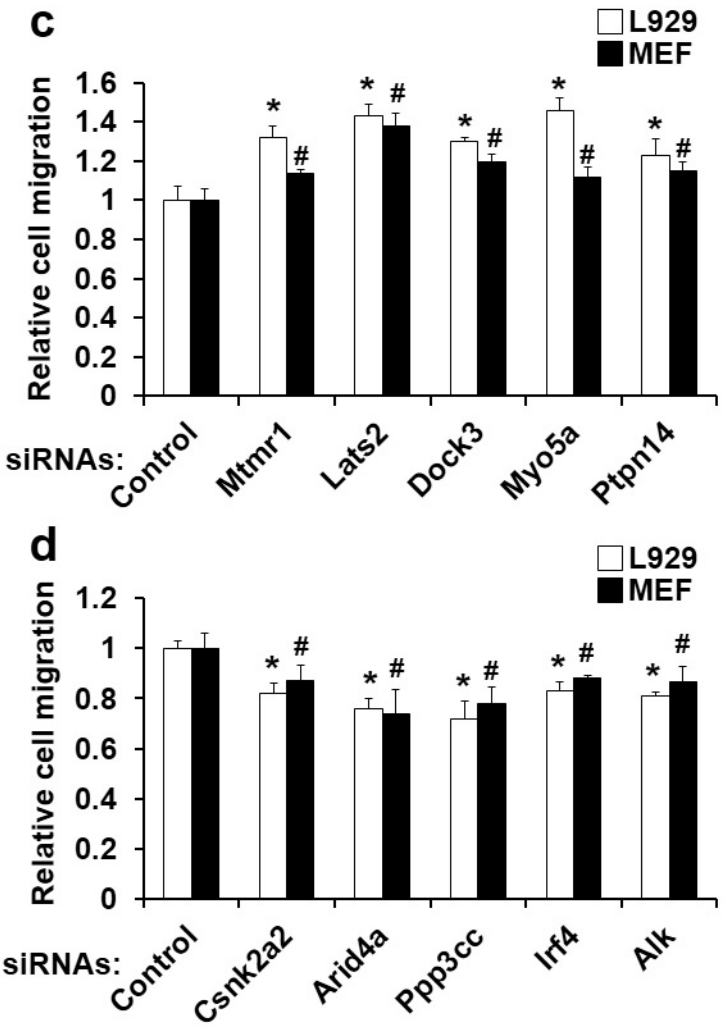

Figure 4. Validation of shRNA hits by three-dimensional cell migration assay.

(**a, b**) NIH3T3 fibroblast cells were transiently transfected with siRNAs targeting cell migration inhibitors (**a**) or promoters (**b**). One siRNA was used for each target: *mtmr1* (#5), *lats2* (#3), *dock3* (#1), *myo5a* (#3), *ptpn14* (#5), *csnk2a2* (#1), *arid4a* (#1), *ppp3cc* (#3), *irf4* (#4), or *alk* (#3). #1 to #5 indicate the siRNAs used for validation in Fig 3. After 24 hr of transfection, NIH3T3 fibroblast cells (4×10^4 cells/well) were seeded onto transwell inserts and incubated at 37°C for 6 hr (**a**; cell migration-accelerating siRNAs) or 9 hr (**b**; cell migration-impairing siRNAs). Non-migrated cells were removed from the upper face of the transwell insert using a cotton swab. Cells that migrated through membranes were stained and counted in 5 randomly selected fields. The results are representative of three independent experiments (*left*) or means ± SDs ($n = 3$) (*right*). *$p < 0.05$ represents significantly different from control siRNA-transfected NIH3T3 cells. Scale bar = 200 μm. (**c, d**) L929 fibroblast cells or mouse embryonic fibroblasts (MEF) were transiently transfected with cell migration-accelerating (**c**) or impairing (**d**) siRNAs identified from the screen. After 24 hr of transfection, L929 or MEF cells (4×10^4 cells/well) were seeded onto the transwell culture inserts and incubated at 37°C for 6 - 9 hr. After incubation, nonmigrated cells were removed from the upper face of the transwell culture insert using a cotton swab.

The cells that migrated across the membrane were stained and counted as described in the main text. The results are mean ± SD ($n = 3$). *$p < 0.05$ represents significantly different from control siRNA-transfected L929 cells. #$p < 0.05$ represents different from control siRNA-transfected MEF cells.

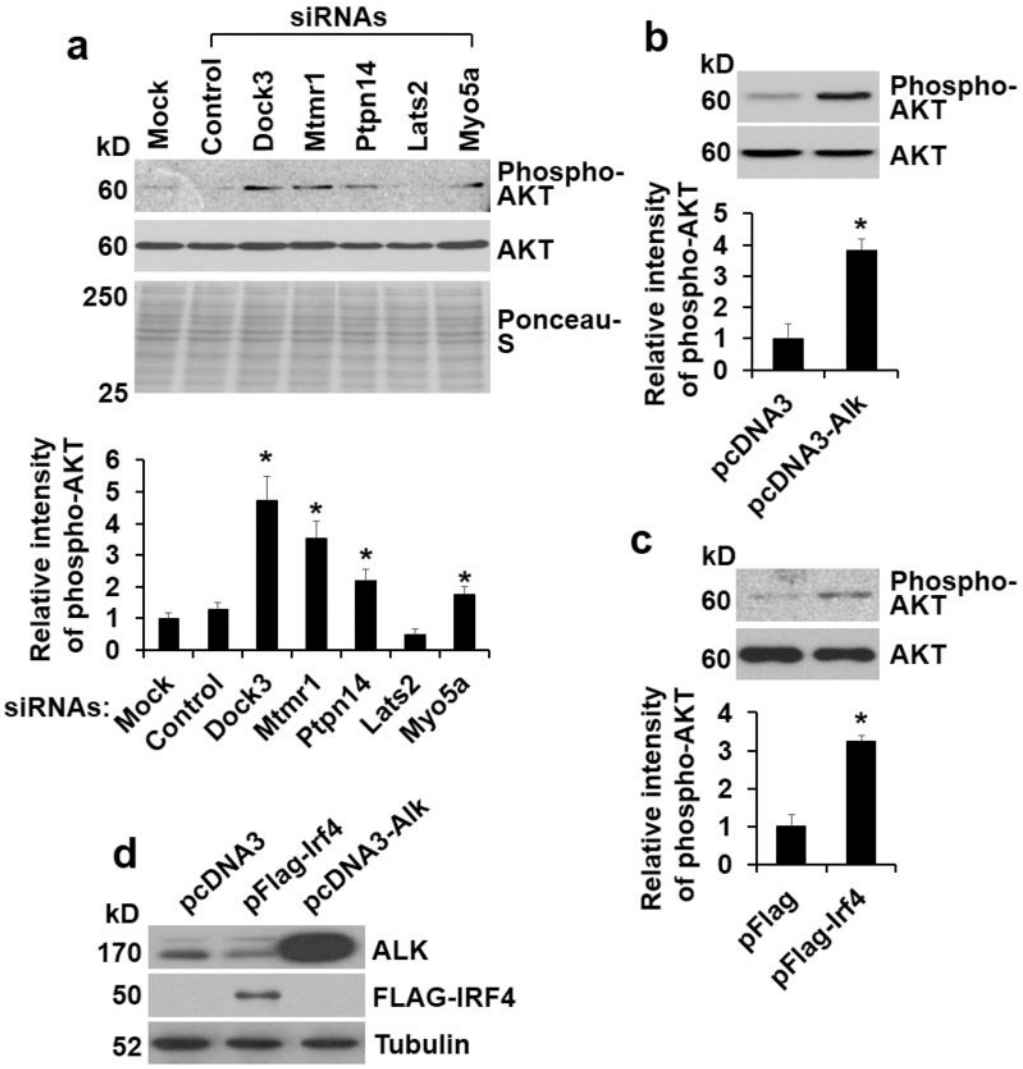

Figure 5. Induction of AKT activation by the selected cell migration regulators.

NIH3T3 fibroblast cells were transiently transfected with control siRNA, siRNAs against *dock3* (#1), *mtmr1* (#5), *ptpn14* (#5), *lats2* (#3), or *myo5a* (#3) (**a**) or empty vectors (*pcDNA3* or *pFlag*), *alk* or *irf4* expression constructs (*pcDNA3-alk* or *pFlag-irf4*) (**b,c**). After 48 hr, levels of phosphorylated AKT (phospho-AKT at Ser473) or total AKT protein were evaluated by Western blot analysis (*upper*). Ponceau S staining was performed to confirm equal sample loading. The results of densitometric analysis are also shown (*lower*). The results shown are means ± SDs ($n = 3$); *p values of < 0.05 indicate significantly different from control siRNA- or empty vector-transfected cells. (**d**) Overexpression of ALK or IRF4 in transfectants was confirmed by Western blotting using anti-ALK or -FLAG-tag antibody. Tubulin was used as the internal control.

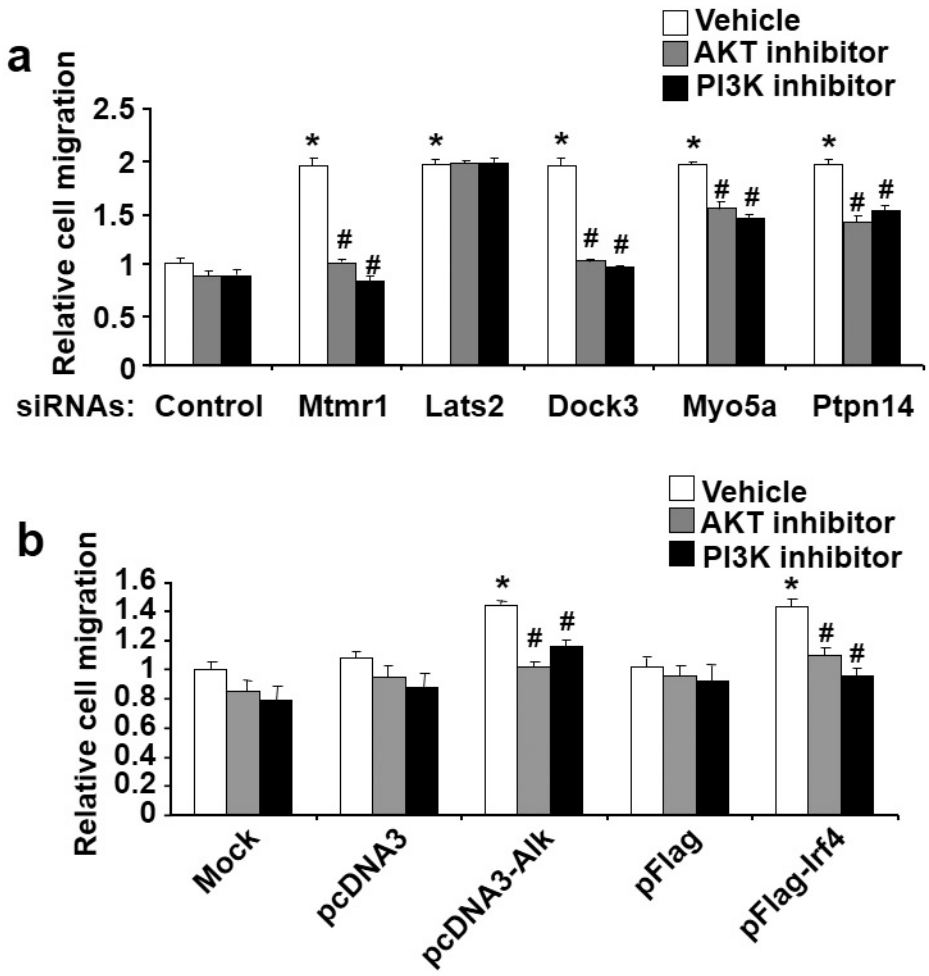

Figure 6. Dependences of selected cell migration regulators on the PI3K/AKT pathway.

(**a**) NIH3T3 cells were transiently transfected with control siRNA or siRNAs targeting *mtmr1* (#5), *lats2* (#3), *dock3* (#1), *myo5a* (#3), or *ptpn14* (#5). After 24 hr, wound-healing assay was conducted and cell migration was quantified in the presence or absence of AKT inhibitor (5 μM) or PI3K inhibitor (LY294002; 15 μM). The results shown are means ± SDs ($n = 3$). * p values of < 0.05 indicate significantly different from control siRNA-transfected cells; # p values of < 0.05 indicate significantly different from the corresponding siRNA-transfected cells not treated with inhibitor. (**b**) Alternatively, NIH3T3 cells were transiently transfected with empty vector (*pcDNA3*) or *alk* or *irf4* expression constructs (*pcDNA3-alk* or *pFlag-irf4*) for 24 hr. Wound-healing assay was performed to evaluate cell migration in the presence or absence of AKT inhibitor (5 μM) or PI3K inhibitor (LY294002; 15 μM). The results shown are means ± SDs ($n = 3$). * p values of < 0.05 indicate significantly different from *pcDNA3* or *pFlag* empty vector transfected cells; # p values of < 0.05 indicate significantly different from the cells under a similar condition without the inhibitor treatment.

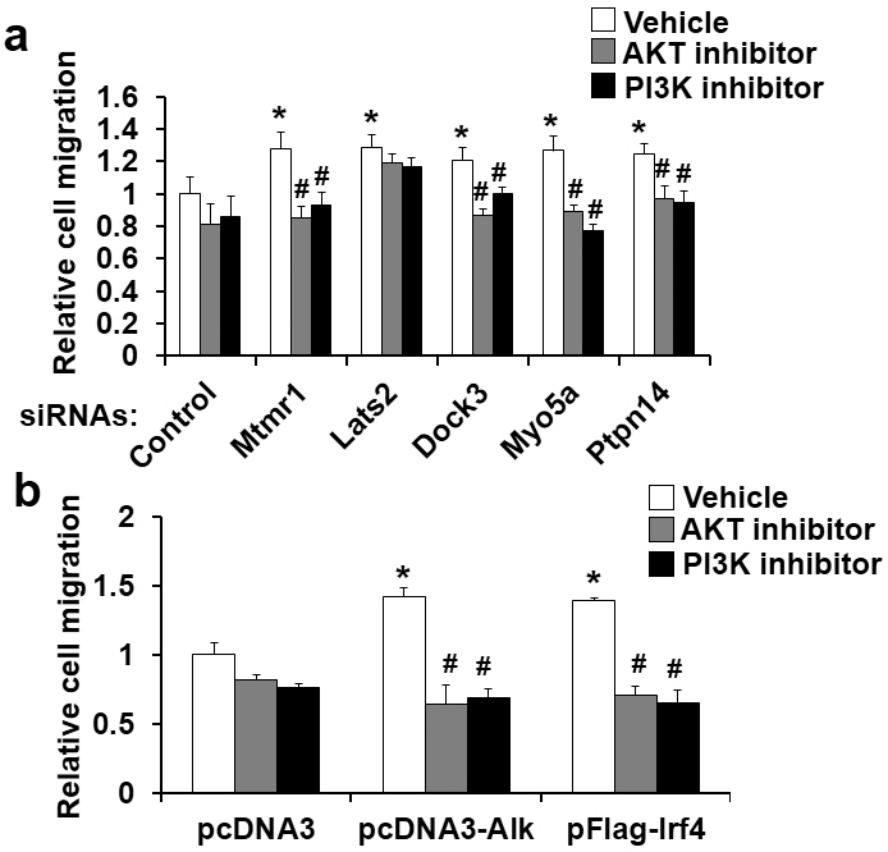

Figure 7. Dependence of selected cell migration regulators on PI3K/AKT pathway determined by three-dimensional cell migration assay.

NIH3T3 cells were transiently transfected with either siRNAs targeted for *mtmr1*, *lats2*, *dock3*, *myo5a*, and *ptpn14* (**a**) or *alk* and *irf4* expression constructs (*pcDNA3-alk* or *pFlag-irf4*) (**b**). After 24 hr of transfection, NIH3T3 fibroblast cells (4×10^4 cells/well) were seeded onto the transwell culture inserts and incubated in the presence or absence of either AKT inhibitor (5 μM) or PI3K inhibitor (LY294002; 15 μM) at 37°C for 6 hr. After incubation, nonmigrated cells were removed from the upper face of the transwell culture insert. The cells that migrated across the membrane were stained and counted as described in the main text. The results are mean ± SD ($n = 3$). $^*p < 0.05$ represents significantly different from control siRNA-transfected cells; $^{\#}p < 0.05$ represents significantly different from the corresponding siRNA-transfected cells without the inhibitor treatment.

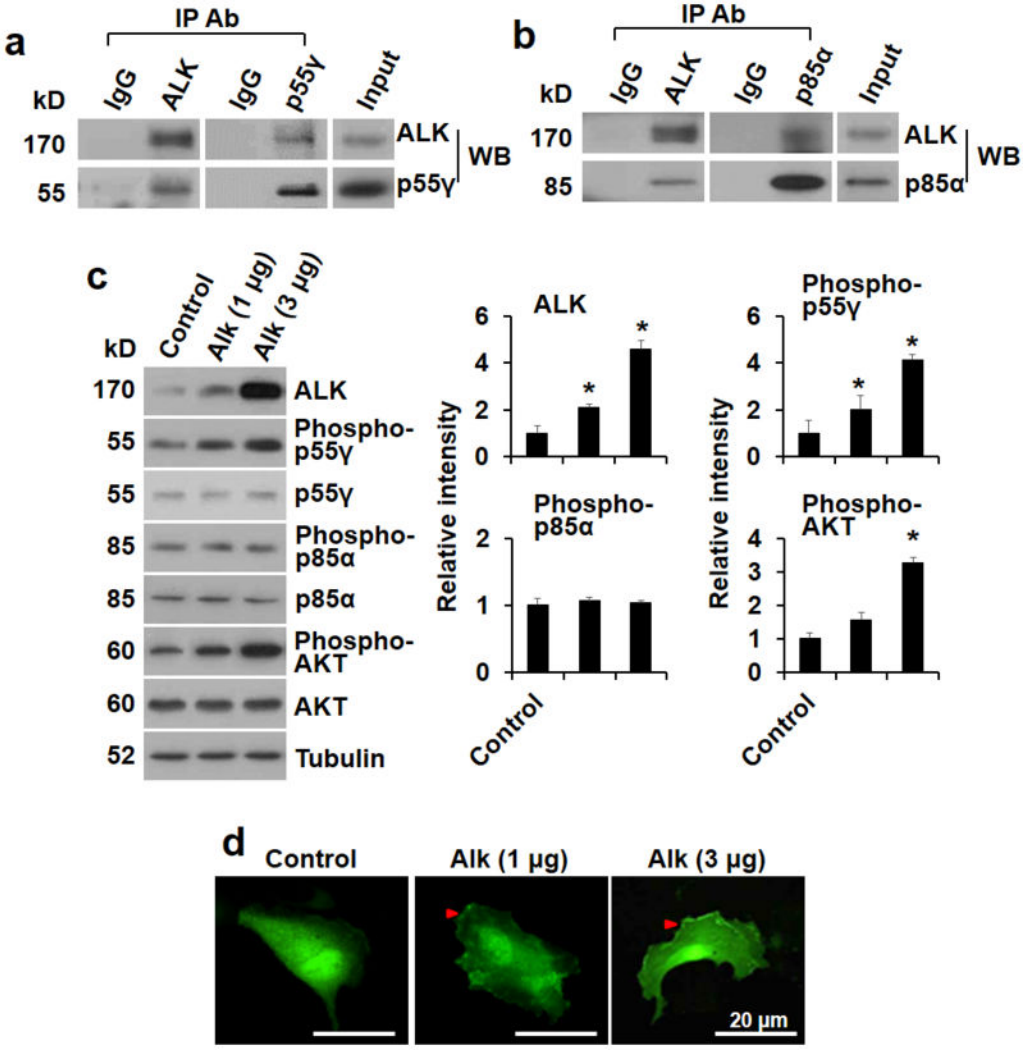

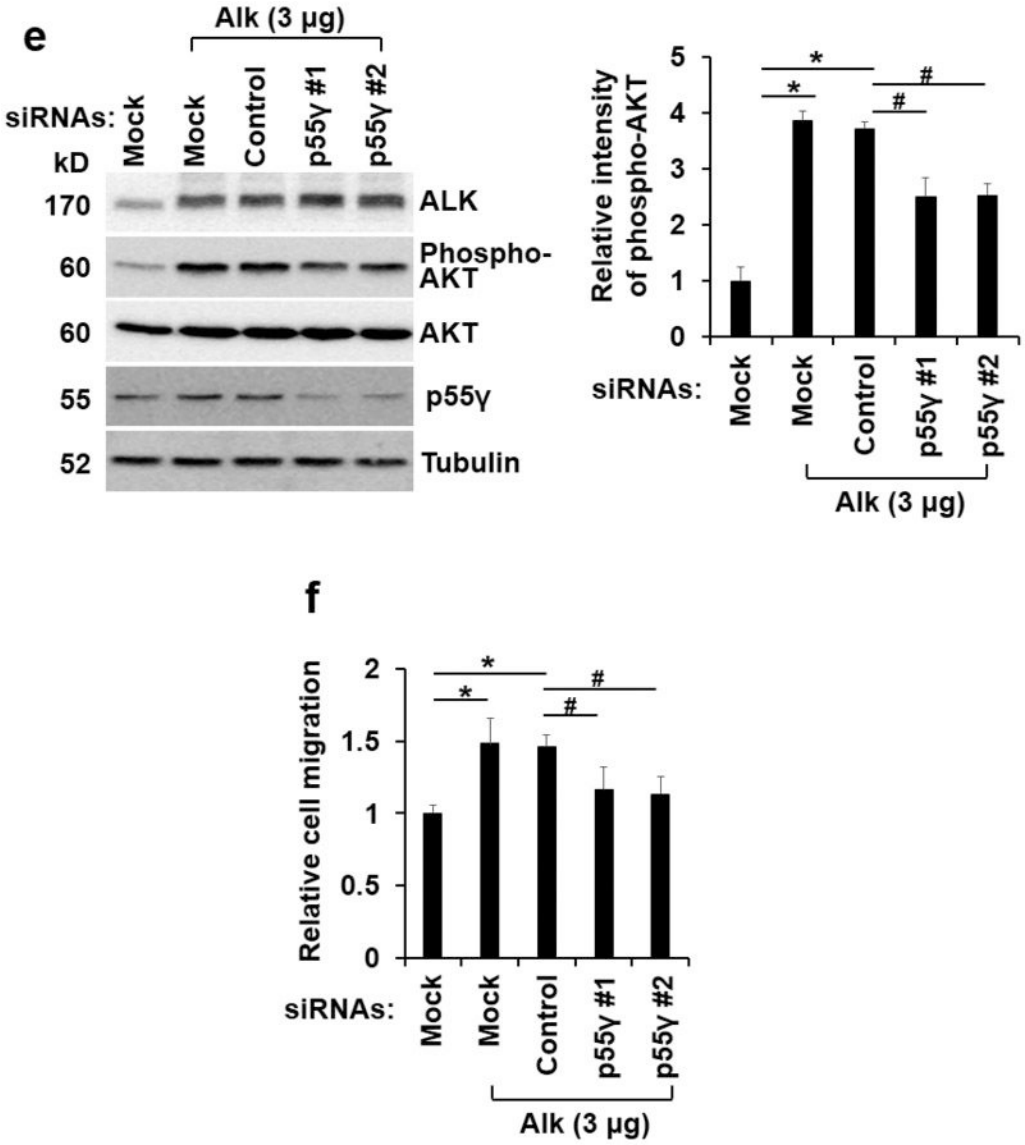

Figure 8. Pivotal role of p55γ subunit of PI3K in Alk-mediated cell migration.

(**a,b**) NIH3T3 fibroblast cells were used to reciprocally immunoprecipitate (IP) with anti-ALK and anti-PI3K antibodies as indicated. Precipitated protein was separated on SDS-PAGE and subjected to reciprocal Western blot analysis (WB) using each antibody. (**c**) NIH3T3 fibroblast cells were transiently transfected with control vector (*pcDNA3*) or *alk* expression constructs (*pcDNA3-alk*). After 48 hr, levels of phosphorylated or total ALK, p55γ, p85α, and AKT were evaluated by Western blotting. Tubulin was used as a loading control. The results of densitometric analysis (*right*) are means ± SDs ($n = 3$); * p values of < 0.05 indicate significantly different from control vector-transfected cells. (**d**) NIH3T3 fibroblast cells on coverslips were transiently transfected with GFP-*akt*-PH expression construct and control vector (*pcDNA3*) or *alk* expression constructs (*pcDNA3-alk*). After 36 hr, transfected NIH3T3 fibroblast cells images were obtained using fluorescence microscopy to determine the localization of the GFP-AKT-PH. Arrowheads indicate plasma membrane-localized GFP-AKT-PH. Scale bar = 20 μm. (**e**) ALK-overexpressing NIH3T3 fibroblast

cells were transiently transfected with control siRNA or siRNAs against *p55γ*. After 48 hr, levels of total or phosphorylated AKT, ALK, and p55γ were evaluated by Western blotting. Tubulin was used as a loading control. The results of phospho-AKT densitometry (*right*) are means ± SDs ($n = 3$). (**f**) After 24 hr of transfection, NIH3T3 fibroblast cells (4×10^4 cells/well) were seeded onto the transwell culture inserts and incubated at 37°C for 9 hr. The cells that migrated across the membrane were stained and counted as described in the main text. The results shown are means ± SDs ($n = 3$); * p values of < 0.05 indicate significantly different from empty vector-transfected cells. # p values of < 0.05 indicate significantly different from control siRNA-transfected cells.

Table 1.

List of shRNAs that accelerated cell migration (with targets genes inhibiting cell migration).

shRNAs were categorized by biological function using DAVID (Database for Annotation, Visualization and Integrated Discovery).

Symbols	Target genes	GenBank accession No.
Cell Cycle		
dgkz	Diacylglycerol kinase zeta	NM_138306
Cell Morphology		
dock3	Dedicator of cyto-kinesis 3	NM_153413
myo5a	Myosin VA	NM_010864
Cell Signaling		
ppid	Peptidylprolyl isomerase D (cyclophilin D)	NM_026352
Cellular Development		
acvr1	Activin A receptor, type 1	NM_007394
cdk13	Cyclin-dependent kinase 13	NM_027118
Inflammatory Response and Disease		
enpp2	Ectonucleotide pyrophosphatase/ phosphodiesterase 2	NM_001136077
gfra2	Glial cell line derived neurotrophic factor family receptor alpha 2	NM_008115
icam2	Intercellular adhesion molecule 2	NM_010494
lats2	Large tumor suppressor 2	NM_015771
Inflammatory Response and Disease		
ptpn14	Protein tyrosine phosphatase, non-receptor type 14	NM_008976
h2-Q10	Histocompatibility 2, Q region locus 10	BC042572
Molecular Transport		
pcyt1a	Phosphate cytidylyltransferase 1, choline, alpha isoform	NM_009981
pts	6-pyruvoyl-tetrahydropterin synthase	NM_011220
Post-Translational Modification		
sbf2	SET binding factor 2	NM_177324
Other/unknown		
A930006J02Rik	RIKEN cDNA A930006J02 gene	AK020818
atmin	ATM interactor	NM_177700
cntnap4	Contactin associated protein-like 4	NM_130457
coro1b	Coronin, actin binding protein 1B	NM_011778
D630033O11Rik	RIKEN cDNA D630033O11 gene	XM_001001707
gabra4	Gamma-aminobutyric acid A receptor, subunit alpha 4	NM_010251
gm379	Gm379 predicted gene 379	XM_142052
gm1971	Gm1971 predicted gene 1971	XM_001472879
gm5615	Predicted gene 5615	NM_001033783
gm12273	Gm12273 predicted gene 12273	XM_001479118
gnal	Guanine nucleotide binding protein, alpha stimulating, olfactory type	NM_010307
gpkow	G patch domain and KOW motifs	NM_173747

Symbols	Target genes	GenBank accession No.
itpripl2	Inositol 1,4,5-triphosphate receptor interacting protein-like 2	NM_001033380
lair1	Leukocyte-associated Ig-like receptor 1	NM_001113474
LOC668961	LOC668961 spindlin 2 family member	XM_001006595
mia3	Melanoma inhibitory activity 3	NM_177389
mpc1	Mitochondrial pyruvate carrier 1	NM_018819
mtmr1	Myotubularin related protein 1	NM_016985
otud6b	OTU domain containing 6B	NM_152812
ptpn3	Protein tyrosine phosphatase, non-receptor type 3	NM_011207
ptpn23	Protein tyrosine phosphatase non-receptor type 23	NM_001081043
ptx4	Pentraxin 4	NM_001163416
rfpl4	Ret finger protein-like 4	NM_138954
trim59	Tripartite motif-containing 59	NM_025863
trip10	Thyroid hormone receptor interactor 10	NM_134125
usp45	Ubiquitin specific peptidase 45	NM_152825
zbed3	Zinc finger, BED domain containing 3	NM_028106

Table 2.

List of shRNAs that impaired cell migration (with targets genes promoting cell migration).

shRNAs were categorized by biological function using DAVID (Database for Annotation, Visualization and Integrated Discovery).

Symbols	Target genes	GenBank accession No.
Cell Cycle		
clip1	CAP-GLY domain containing linker protein 1	NM_019765
Cell Morphology		
actg1	Actin, gamma, cytoplasmic 1	NM_009609
add1	Adducin 1 (alpha)	NM_001024458
akt3	V-akt murine thymoma viral oncogene homolog 3 (protein kinase B, gamma)	NM_011785
des	Desmin	NM_010043
itgb8	Integrin beta 8	NM_177290
pik3ca	Phosphoinositide-3-kinase, catalytic, alpha polypeptide	NM_008839
rdx	Radixin	NM_009041
sep15	Selenoprotein	NM_053102
sorbs1	Sorbin and SH3 domain containing 1	NM_001034962
tpm3	Tropomyosin 3,gamma	NM_022314
vim	Vimentin	NM_011701
Cell Signaling		
apc	Adenomatosis polyposis coli	NM_007462
Cellular Assembly and Organization		
adam2	A disintegrin and metallopeptidase domain 2	NM_009618
Cellular Development		
alk	Anaplastic lymphoma kinase (Ki-1)	NM_007439
irf4	Interferon regulatory factor 4	NM_013674
igf1r	Insulin-like growth factor 1 receptor	NM_010513
Cellular Movement		
abl1	V-abl Abelson murine leukemia viral oncogene homolog 1	NM_009594
abl2	V-abl Abelson murine leukemia viral oncogene homolog 2 (arg, Abelson-related gene)	NM_001136104
arhgap5	Rho GTPase activating protein 5	NM_009706
csnk1a1	Casein kinase 1, alpha 1	NM_146087
csnk2a2	Casein kinase 2, alpha prime polypeptide	NM_009974
irgm1	Immunity-related GTPase family M member 1	NM_008326
itgav	Integrin, alpha V (vitronectin receptor, alpha polypeptide, antigen CD51)	NM_008402
nrp2	Neuropilin 2	NM_001077403
pak4	p21 protein (Cdc42/Rac)-activated kinase 4	NM_027470
Metabolism		
abi2	Abl interactor 2	NM_001198570
mogat1	Monoacylglycerol O-acyltransferase 1	NM_026713
Other/unknown		

Symbols	Target genes	GenBank accession No.
akap11	A kinase (PRKA) anchor protein 11	NM_001164503
arhgap26	Rho GTPase activating protein 26	NM_175164
arid4a	AT rich interactive domain 4A (RBP1-like)	NM_001081195
ccdc34	Coiled-coil domain containing 34	NM_026613
cdc42	Cell division cycle 42 (GTP binding protein, 25kDa)	NM_009861
cdh12	Cadherin 12, type 2 (N-cadherin 2)	NM_001008420
cmtm2b	CKLF-like MARVEL transmembrane domain containing 2B	NM_028524
defb20	Defensin beta 20	NM_176950
eif3e	Eukaryotic translation initiation factor3, subunit E	NM_008388
frmd6	FERM domain containing 6	NM_028127
g3bp2	Ras-GTPase activating protein SH3 domain-binding protein 2	NM_001080794
gpr143	G protein-coupled receptor 143	NM_010951
hpdl	4-hydroxyphenylpyruvate dioxygenase-like	NM_146256
hsd17b11	Hydroxysteroid (17-beta) dehydrogenase 11	NM_053262
pdgfrl	Platelet-derived growth factor receptor-like	NM_026840
ppp3cc	Protein phosphatase 3, catalytic subunit, gamma isoform	NM_008915
rnf139	Ring finger protein 139	NM_175226
rp17	Ribosomal protein L7	NM_011291
stradb	STE20-related kinase adaptor beta	NM_172656
svil	Supervillin	NM_178046
tm4sf5	Transmembrane 4 superfamily member 5	NM_029360